# Chapter 2
# The Retinal Processing of Photoreceptor Signals

**Jan Kremers, Luiz Carlos L. Silveira, Neil R.A. Parry, and Declan J. McKeefry**

**Abstract** Color vision is the ability to perceive differences in the wavelength content of a light source, a process which starts with absorption of photons of different wavelengths and energies by the photopigments. In this chapter, the photopigments and the efficiency with which light of different wavelengths are absorbed by a photopigment are discussed. In addition, the translation of a photoisomerization to a photoreceptor excitation is considered as well as the signal transmission from the photoreceptors to post-receptoral cells and the post-receptoral processing of this signal in the retina. A large part of the chapter provides an overview of recent evidence that retinal processes in the major retino-geniculate pathways that are

J. Kremers, Ph.D. (✉)
Department of Ophthalmology, University Hospital Erlangen, Schwabachanlage 6, 91054 Erlangen, Germany

School of Optometry and Vision Science, University of Bradford, Richmond Road, Bradford, West Yorkshire BD7 1DP, UK
e-mail: Jan.kremers@uk-erlangen.de

L.C.L. Silveira, Ph.D. (deceased)

N.R.A. Parry, Ph.D.
School of Optometry and Vision Science, University of Bradford, Richmond Road, Bradford, West Yorkshire BD7 1DP, UK

Centre for Hearing and Vision Research, Institute of Human Development, University of Manchester, Manchester, UK

Vision Science Centre, Manchester Royal Eye Hospital, Central Manchester University Hospitals NHS Foundation Trust, Manchester Academic Health Science Centre, Manchester, UK
e-mail: neil.parry@manchester.ac.uk

D.J. McKeefry, Ph.D.
School of Optometry and Vision Science, University of Bradford, Richmond Road, Bradford, West Yorkshire BD7 1DP, UK
e-mail: d.mckeefry@bradford.ac.uk



J. Kremers et al. (eds.), *Human Color Vision*, Springer Series in Vision Research, DOI 10.1007/978-3-319-44978-4_2

relevant for luminance and color vision, can be studied in the intact visual system by electroretinography (ERG), thus providing the possibility of direct study of human retinal physiology.

**Keywords** Photopigments • Fundamentals • Photoreceptors • Retinal pathways • Electroretinography • Silent substitution • Horizontal cells • Bipolar cells • Retinal ganglion cells • Post-receptoral circuitry • Cone opponency

## 2.1 Photopigments and Excitation of Photoreceptors

### *2.1.1 Spectral Sensitivities of Photopigments and Fundamentals*

Photoreceptors are neurons that are specialized for the absorption of light and transforming light information into electrical signals. Signals that are further processed in the retina and transmitted to the brain for visual perception and non-conscious behaviors such as eye movements, pupillary reflexes, and circadian rhythms. The chromophore, an aldehyde of vitamin A called retinal, and the opsin protein, which is an integral protein of the plasma membrane, together form the photopigment. The visual response starts with absorption of photons by the photopigments resulting in an isomerization of the retinal chromophore. Retinal isomerization triggers a cascade of internal changes that finally leads to photoreceptor hyperpolarization, as a result of changes in ion transfer across the cell membrane thanks to opening and closing of the ion pores controlled by the chromophore. Unlike most other neurons, photoreceptors (and the majority of other retinal neurons except retinal ganglion cells) do not propagate electrical signals through action potentials, but do so instead via graded potential changes.

The absorption of a photon leads to deformation or photo-isomerization of the retinal chromophore from the 11-*cis*- to the all-*trans*-configuration. The photopigments are mainly present in the photoreceptors but some retinal ganglion cells contain melanopsin and as a result are also photoresponsive [1–6]. These recently discovered intrinsically photosensitive ganglion cells (ipRGCs) are thought to have little or no role in vision (but see Ecker et al. [7] for a challenging idea) and are probably not involved in color vision. They are therefore not considered in depth in this chapter.

### *2.1.2 Variability of Pigment Spectra and Its Consequences for Psychophysics*

The Principle of Univariance [8] states that the effect of every photon that is absorbed is the same, independent of the wavelength or energy content of the photon. Thus, a photoisomerization always leads to the same configuration change

of the retinal chromophore as mentioned above and to the same response (i.e., hyperpolarization) of the photoreceptor.

Importantly, the chance that a photon is absorbed and that a photoisomerization takes place is not always the same and depends on the wavelength of the light. The probability of a photoisomerization as a function of wavelength is described by the absorption spectrum. The absorption spectrum is determined by the properties of the retinal and the amino-acid sequence of the opsin protein in which the retinal is embedded. In humans, there are three types of cone opsin, the configurations of which are genetically determined. The genes for the L- and M-cone opsins are located on the X-chromosome. The gene for S-cone opsins is located on chromosome 7 (see Chap. 1). In situ, the absorption spectrum is also influenced by other parameters such as pigment concentration and length of the photoreceptor outer segments. These factors influence the absorption spectrum through self-screening effects. The photopigment is ordered in layers in the stacks of membranes in the photoreceptor outer segments. The first layer absorbs more light with wavelengths close to the maximum of its spectral sensitivity. As a result, the light reaching the second layer contains less photons with wavelengths close to this maximum (the first layers is thus screening the second layer) and therefore will also absorb less light close to maximum and more of the "submaximal" wavelengths in comparison with the first layer. This self-screening effect is propagated through all layers. The overall absorption spectrum thus will become broader the more layers the light will have to pass.

In order to be able to appreciate the effect of light with a certain wavelength content, the absorption spectrum alone is generally not sufficient to provide all the necessary information. For many cases and experimental situations (basically those in which measurements are performed with intact eyes), pre-retinal absorption (mainly by the cornea and the lens) alters the wavelength content of light reaching the retina. In these cases, not the rod and cone absorption spectra but the rod and cone fundamentals, that include pre-retinal absorption, should be taken into account. The fundamentals therefore describe the efficiency of light at the level of the pupil entrance of the eye to stimulate the photoreceptors. Figure 2.1 shows the fundamentals of the human photoreceptors. The most often used fundamentals are those of Smith and Pokorny [9, 10] and of Stockman and colleagues [11–14] (see Chap. 5).

The absorption spectra are more appropriate than the fundamentals when considering the results of in vitro or ex vivo experiments (in which the retina has been excised from the eye or pre-retinal tissue has been removed).

### *2.1.3 Responses of Photoreceptors to Stimuli*

The efficiency with which a stimulus is able to excite a photopigment is calculated by the multiplication of the fundamentals with the emission spectrum of the stimulus integrated over the wavelength range. Following the Principle of Univariance, the photopigment excitation is proportional to the response (hyperpolarization) of the photoreceptor and thus describes the sensitivity of the photoreceptor to the stimulus.

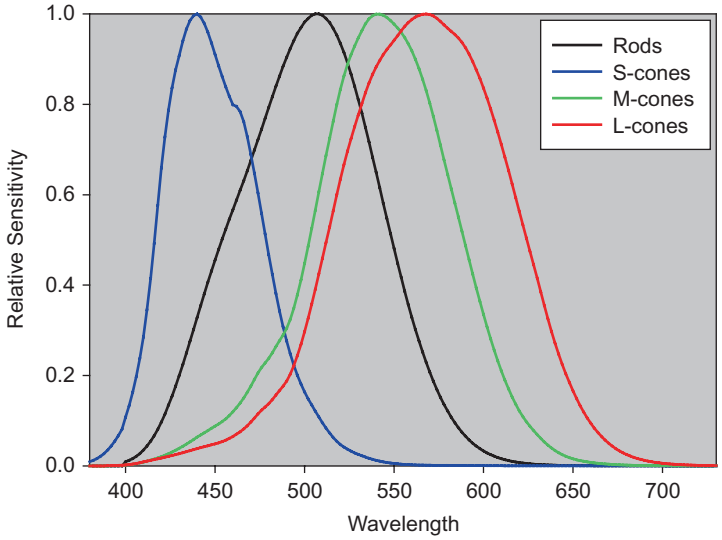


**Fig. 2.1** Normalized cone [11, 14] and rod fundamentals. The fundamentals describe the sensitivity of the different photoreceptor types for stimulation at the pupil. The sensitivities are normalized to unity at their maxima. The rod fundamental is identical to the scotopic spectral luminosity function [$V'_\lambda$; [15]]. The cutoff at short wavelengths is caused by pre-retinal absorption mainly by the lens and the cornea

Sensitivity is defined as the inverse of the stimulus strength required to evoke a criterion response or a psychophysical threshold. Alternatively, particularly in physiological experiments, sensitivity can be quantified by a gain that is defined as the change in response amplitude caused by a change in stimulus strength (i.e., the slope of the response amplitude vs. stimulus strength curve). Crucially, however, the photoreceptors are dynamic, changing their sensitivity via adaptation when the stimulus is strong, or presented over an extended time.

The strength of a repetitive stimulus around a mean level is quantified by Michelson contrast (*MC*):

$$\mathrm{MC} = \frac{E_{\max} - E_{\min}}{E_{\max} + E_{\min}}$$

where $E$ is the cone or rod excitation (or photoreceptor sensitivity), $E_{\max}$ and $E_{\min}$ are the maximal and minimal excitations, respectively. Observe that the same formula is also used to calculate luminance contrast where $E$ is replaced by the luminance. The luminance is calculated in a similar manner as $E$ with the difference that instead of the fundamentals, the emission spectra are multiplied by the photopic spectral luminosity function, $V_\lambda$, This definition of stimulus strength is useful when the modulation of the excitation is evenly distributed around the mean level (such as in sine-wave or square-wave stimuli). In such instances the addition of the two (i.e., $E_{\max} + E_{\min}$) equals twice the mean excitation. The main advantage in using this

metric is that stimulus strength (cone and rod contrast; similarly for luminance contrast) can be changed without changing of the mean level and vice versa.

For pulsed stimuli, Weber contrast (*WC*) is more useful to describe stimulus strength:

$$\mathrm{WC} = \frac{E_{\max} - E_{\min}}{E_{\min}}$$

Here, $E_{\min}$ equals the excitation caused by the background and, for short-lived weak pulses (when $E_{\max} - E_{\min}$ is small in comparison with $E_{\min}$), also the mean excitation. The problem with pulses is that the mean excitation changes with pulse strength and duration. This may cause the visual system to adapt and change its sensitivity.

There are two ways to isolate the responses from a particular photoreceptor type. In the early days of psychophysical studies, when there was no precise knowledge about the fundamentals or the physiological properties of photoreceptors and when the technical possibilities for stimulus presentation were limited, this was achieved by selective desensitization of the photoreceptors that were not of interest by a background and selective isolation of the photoreceptor under study with a flash stimulus [12, 16, 17] (See also Ch. 5).

Although a well-established technique, this method of selective desensitization has its disadvantages. First, complete isolation is difficult, if not impossible, to achieve, particularly when flash and background wavelengths are not very different. Second, the abovementioned disadvantages of pulsed stimuli also count here. Third, to study different photoreceptor types, different backgrounds need to be used which induce different states of adaptation in the retina and the visual system. This may affect the outcome of the measurements and the results from different photoreceptor isolation conditions cannot therefore be easily compared.

An alternative is the silent substitution method using periodic stimuli around a mean luminance and chromaticity (Fig. 2.2). This method was first introduced by Donner and Rushton [18] and further developed by Estévez and Spekreijse [19, 20]. With the technical advance of cost-effective stimulus devices that can deliver stimuli with well-defined spectral, temporal, and spatial properties, this method has become extremely attractive and has now generally replaced the method of selective adaptation. The silent substitution method can be applied to flashed and to continuously modulating stimuli. In the latter case, as mentioned before, the state of adaptation can be kept constant even when different mechanisms are studied. Furthermore, isolation of the responses of different photoreceptor types can, at least theoretically, be more complete than with the selective adaptation method [21]. A silent substitution is the replacement of one stimulus by another of different spectral composition. It is possible to choose the luminance (intensity) of the two stimuli so that the number of photoisomerizations in one photoreceptor type, and thus its excitation, does not change (and cone or rod contrast, as defined above, equals zero). The principle is illustrated in Fig. 2.2 for two monochromatic stimuli and two hypothetical photopigments. The number of photoisomerizations depends on the fundamentals of the photoreceptors and on the intensity of the stimuli. In Fig. 2.2 the number of photoisomerizations of the two hypothetical photoreceptor types, containing

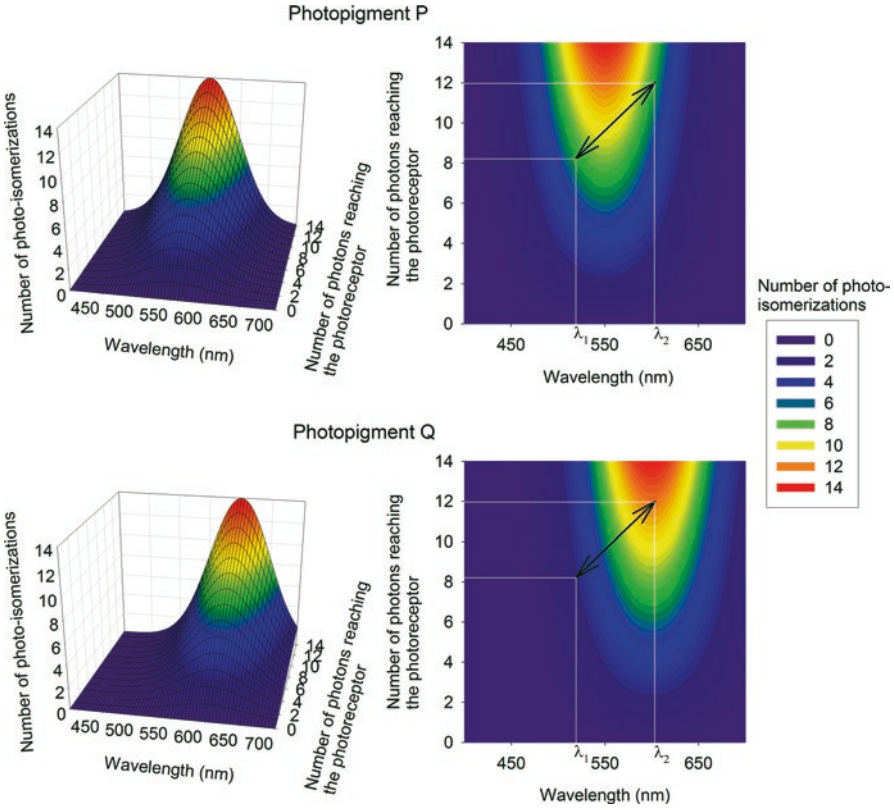


**Fig. 2.2** Explanation of the silent substitution method. The numbers of photoisomerizations in two photoreceptor types with different photopigments (P and Q) are given as function of wavelength and intensity of the stimuli. The effect of wavelength is described by the fundamental. Stimulus intensity is assumed to have linear effect: if the intensity is doubled, the number of isomerizations is also doubled. In the *right plot* an example of a stimulus (an exchange between two monochromatic lights, $\lambda_1$ and $\lambda_2$) is shown. The intensity of the two lights is chosen to counteract the difference in probability of an absorption of a photon in photopigment P as described by the fundamentals. As a result, the number of isomerizations does not change by the wavelength exchange. This stimulus results in a silent substitution for photoreceptor P and the isolation of the response of photoreceptor Q. Reprinted with permission from Kremers [21]

photopigments P and Q, are given as a function of wavelength and of intensity. Three dimensional plots are given on the left. On the right, the same is displayed in a color coded manner. The double headed arrows signify a modulation between two monochromatic stimuli ($\lambda_1$ and $\lambda_2$). The intensities of these two stimuli are chosen such that the number of photoisomerizations in photopigment P (and thus the excitation of the photoreceptor containing photopigment P) is not altered. The stimulus is a silent substitution of that photoreceptor. The number of photoisomerizations in photopigment Q is strongly altered. Only the photoreceptor containing photopigment Q responds to the stimulus and thus is isolated.

The silent substitution method can be extended to stimuli with broadband and complex emission spectra, such as LEDs or CRT monitors. The method is not only suitable for silencing one or more photoreceptor types, but also allows the choice of any stimulus strength for each photoreceptor type, provided the stimuli are within the gamut of the stimulator. The number of photopigments that can be independently stimulated can be increased when more light sources are used. Theoretically, the number of independent light sources should at least equal the number of photopigments present. Since humans have normally four different photoreceptor types, a four primary stimulator is necessary [22]. If the melanopsin pigment also has to be taken into account, a five primary stimulator is desirable [23].

In practice, the silent substitution method may be contaminated by errors, miscalculations, misinterpretations, and oversimplifications. For instance macular pigment, which only covers the central retina, influences pre-retinal absorption and as a consequence will affect the wavelength composition of light reaching the photoreceptors differently in the central compared to the peripheral retina. Furthermore, individual differences in the optical density of the macular pigments [24, 25] result in individual differences in central cone fundamentals. It is often difficult to take this spatial and individual variability into account in psychophysical and physiological measurements. However, as work with dichromats and other control experiments have often shown [26–29], the silent substitution method is generally very effective. For instance, the isolation of L-cone driven responses can be tested in protanopes who lack the L-cones. Stimuli that isolate L-cones elicit electrophysiological responses and psychophysically measured perception in trichromats and deuteranopes but not in protanopes. Similarly, M-cone isolating stimuli elicit much smaller responses in deuteranopes (they are not always completely abolished; we return to this issue later). Rod isolating stimuli elicit small ERG responses when full field stimuli and high luminances are used. At low luminances and with smaller stimuli, the rod responses are increased in amplitude through stimulation of the dark adapted surrounding retina through stray light (McKeefry, Maguire, Parry, Murray, Kommanapalli, Aher, Kremers unpublished data; see also Park et al. [30]). In psychophysical experiments, the degree of rod isolation can be tested by bleaching the rods prior to the measurements. If only rods are stimulated, the stimuli should not be perceivable directly after bleaching. Perception of the stimuli should return only after several minutes of dark adaptation. Cone-driven perception returns to normal much more quickly after bleaching [31].

## 2.2 Physiological Basis of Color Vision

As mentioned above, color vision is the ability to perceive, within limits, the wavelength content of light emitted by a luminous source or reflected by an illuminated surface. Physiologically, there are two prerequisites for color vision. First, photoreceptor types with different absorption spectra are necessary. In humans and under photopic conditions, three different cone types provide the basis for color vision. Depending on the wavelength content of the light reaching the cones, their relative

excitations will be different which will influence the percept of color. Because humans normally have three cone types, color vision is trichromatic: all perceived colors can be obtained by mixing the outputs of three independent primaries (independent in this context means that the output of one of the three primaries cannot be obtained by mixture of the output of the other two). With these cone types, wavelengths between approximately 380 and 780 nm can be distinguished (see Fig. 2.1).

The second prerequisite for color vision is a mechanism that can determine the relative cone excitations. These mechanisms are thus post-receptoral. Probably, multiple comparisons are performed at different stages in the visual system.

## 2.3 Post-receptoral Processing

The signals coming from the photoreceptors are processed in a parallel manner directly at the first synapse, where connections are made with different types of horizontal cells and bipolar cells that have different anatomical and physiological properties.

Color vision can only occur when the relative excitations of the three cone types are determined by post-receptoral processing of cone signals. In the retina, the signals are processed in parallel in different post-receptoral channels or pathways. The main retinal pathways are already separated at the level of the bipolar cells. The properties of the different pathways and signal processing therein are subject of Chap. 4. Here, we summarize the properties with an emphasis on how the signals, originating in the different cone types, are distributed and processed.

Many studies on primate color vision are performed in Old and New World monkeys. New World monkeys are closely related to humans and Old World monkeys but show different photoreceptor phenotypes. Therefore they make it possible to study the relationship between cone phenotypes and retinal wiring and the effect this has on their color vision [32]. Most New World monkeys have only one gene coding for a cone photopigment on the X-chromosome, but there are three or even more alleles of this gene in the population. As a result, color vision is polymorphic with all males and the homozygous females are dichromats whereas the heterozygous females are trichromats. One species, the howler monkey, displays full trichromacy similar to Old World monkeys [33, 34]. However, trichromacy in these species has probably evolved independently [35, 36]. Finally, the nocturnal owl monkeys lack S cones and are therefore obligatory monochromats [37, 38]. These species form natural experiments in which the signals of different photoreceptor types can be studied.

### *2.3.1 Horizontal Cells and Their Connectivity*

Horizontal cells and bipolar cells form the first steps of the neuronal processing of photoreceptor outputs and bipolar cells transmit information from the inner to the outer plexiform layers [32]. Amacrine cells and ganglion cells further process the

photoreceptor signals, whereas inter-plexiform cells transmit information from the inner plexiform layer back to the outer plexiform layer. Ganglion cells send the results of retinal processing to higher visual centers located in the mesencephalon and diencephalon [32]. We refer to Chap. 4 for a more detailed discussion of the responses of retinal ganglion cells and neurons of the lateral geniculate nucleus with respect to cone opponent processing and generation of the information necessary for color perception.

The retinae of all primates so far studied (including humans) have post-receptoral neurons, comprising horizontal cells, bipolar cells, amacrine cells, inter-plexiform cells, and ganglion cells. Their morphologies and functional roles are similar across species. The morphology of these cells, the connections that they make in the inner and outer plexiform layers, and the two-dimensional mosaics they form in the retinal layers have been studied using techniques that stain individual cells [33–35] or cell populations [36–41]. Intracellular injection of neurotracers is a powerful method to study both the morphology of individual cells and the properties of cell populations [42–46].

Primates have two classes of horizontal cells, H1 [33] and H2 [47], whose morphology, cone connectivity, and distribution have been extensively described in humans [47–50] and several diurnal monkeys [45, 51–55] (see Fig. 2.3). H1 and putative H2 horizontal cells have also been described in the single extant nocturnal monkey, the owl monkey, although H2 cells seem to be very rare and exhibit a simple morphology [56]. H1 horizontal cells have large cell bodies and radiate stout primary dendrites bearing conspicuous clusters of terminals which can be traced to axon pedicles of M or L cones. In the majority (85%) of H1 horizontal cells, the dendritic terminals make synapses exclusively with M and L cones. In the other 15%, a few synapses contact S cones [54]. H1 horizontal cells typically have 4 dendritic clusters in the foveal region, increasing to 8 at about 1 mm of eccentricity, and 30 or more at higher eccentricities [49, 55]. From the fovea to the retinal periphery, the inter-cluster distance strictly follows the inter-cone distance, as measured in cone mosaics visualized in retinal flat-mounts [56]. H1 horizontal cells have axons that are thick, run away from the cell body in straight paths for a long distance and then exhibit fan-shaped terminals with compact branches and tiny knobs, which can be traced to rod spherules.

H2 horizontal cells have medium-sized cell bodies and thin, curved, intertwined, profusely branched dendrites with dendritic terminals that, unlike H1 cells, are not clearly organized to form clusters. The dendrites of H2 horizontal cells are directed to contact all cone pedicles—S, M, or L—overlying their dendritic fields. However, S cone pedicles make more synapses with H2 dendrites than M or L cone pedicles do [45] (Fig. 2.3). In an anatomical study of the marmoset retina, about 11% of synapses to a single H2 horizontal cell were formed by a single S cone pedicle which represented only 4% of all cones under the cell dendritic tree [54]. The H2 axons are short and convoluted, branch one or more times, and bear a small number of terminals along their paths that also contact S cone pedicles.

H1 and H2 dendritic trees and H1 axon terminals form three cell networks in the outer plexiform layer extensively coupled by specific types of gap junctions [58–60]. Thus, the response to light of a single horizontal cell occurs in a retinal region much

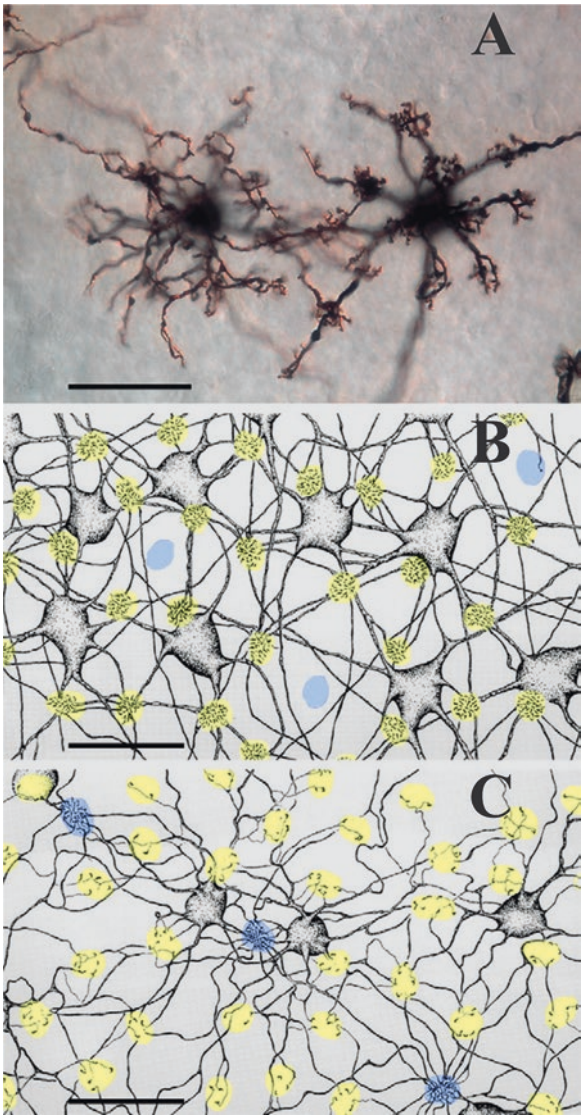


**Fig. 2.3** H1 and H2 horizontal cells and their cone contacts. The morphology, connectivity, and retinal distribution of retinal cells can be studied by combining different techniques to stain individual cells, to label a particular cell population, and to double label the overlying cone mosaic. (**a**) Photomicrograph of macaque H1 and H2 cells stained with the method of Golgi, which uses heavy metals such as silver and mercury compounds to impregnate neurons. Cells are shown in flat view focused on the dendritic trees and terminal dendritic clusters. (**b**) Drawings of macaque H1 cells stained by neurobiotin injection in one of the cells. The tracer diffused to the neighboring H1 cells through gap junctions between them. H1 cells form dense terminal dendritic clusters at all M- and L-cone pedicles (indicated by *yellow patches*), but almost completely miss three S-cones (*blue patches*). (**c**) Drawing of macaque H2 cells similarly labeled with neurobiotin. They form dense terminal dendritic clusters at the three S-cones (*blue*), but also contact the M- and L-cones. Scale bars = 25 μm. Images kindly provided by Dennis Dacey to Leo Peichl. Reproduced with permission from: Peichl, L. [57]

larger than that covered by its processes. The strength of coupling in the cell network is highly dynamic and is modulated by light-dependent changes in the levels of several neuromodulators including dopamine, nitric oxide and retinoic acid [60].This allows horizontal cells to play an important role in the spatial extent of the interactions between photoreceptors and post synaptic interneurons [61]. Horizontal cells send feed-back and feed-forward inhibitory signals to cones and rods and bipolar cells, thereby mediating lateral inhibition. Thus they serve to integrate and control photoreceptor output, allowing the retina to adapt to a broad range of light intensities and contributing to center-surround organization of bipolar and ganglion cells [61].

The difference between the two types of horizontal cells suggests that H2 cells may have a role in the blue-yellow pathway that receives S cone signals. The exact function of horizontal cells in color vision is, however, unclear. Considering the H1 morphologies of trichromatic, dichromatic, and monochromatic Old- and New-World monkeys, there are no major inter-species differences that could be related to their cone phenotypes. This implies that horizontal cells play only a minor role in primate color vision [54–56, 62, 63]. The sparseness and simple morphology of H2 horizontal cells in the retina of the owl monkey is probably related to the absence of S cones [56]. Thus, horizontal cells in primates (and other mammals) seem to exhibit cone specificity without cone opponency [45] (Fig. 2.4). This is in contrast with fish and turtles where horizontal cells seem to be the basis of color vision [64, 65].

### *2.3.2 Bipolar Cells and Their Connectivity*

Primate bipolar cells comprise several morphological classes with specific connections in the outer and inner plexiform layers, and with putatively diverse roles in vision [33, 34, 66–69]. The work of Boycott and Wässle [35] established the current classification of primate bipolar cells. Specific antibodies are now available that selectively label several bipolar cell classes. As a result there is increasing interest in a detailed characterization of primate bipolar cell morphology, spatial distribution, cone connections, and synaptic targets in the inner retina. In spite of the amount of information about individual cells provided by the Golgi method [35] or DiI labeling [70], immunocytochemistry has been particularly critical for the advancement of knowledge on the populations of these small, very numerous, and diversified retinal interneurons [38, 70–72].

The cone signals diverge to several cone bipolar cell classes, suggesting that, at the very first synapse of the visual pathway, visual information is distributed into parallel pathways for further processing. Thus, the identification and characterization of the bipolar cell classes is paramount to understand how parallel processing in the visual system starts and is organized through the retinal layers. Boycott and Wässle [35] described ten different bipolar cell classes in the retina of rhesus macaque, characterizing them by the number of cones or rods they contact with their dendrites, the depth of their cell body in the inner nuclear layer and the shape and level of branching of their axon terminals in the inner plexiform layer. Further

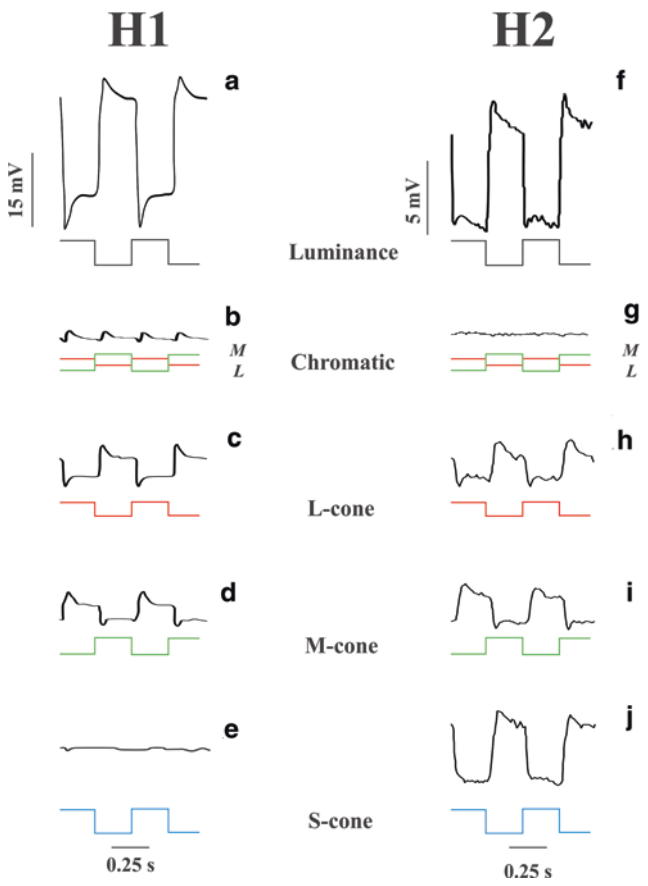


**Fig. 2.4** Electrophysiology of cone inputs to H1 and H2 horizontal cells. Responses of horizontal cells to different stimuli are depicted below each trace. The five rows display responses to luminance (in phase modulation of S-, M-, and L-cones), chromatic (counter-phase modulation of M- and L-cones), and to L-, M-, and S-cone isolating stimuli respectively. H1 cells (*left column*) display sustained hyperpolarizing responses to luminance increments (**a**) and small responses at twice the stimulus frequency to chromatic modulation (**b**). Selective modulation of L- or M-cones also elicits a hyperpolarizing response (**c** and **d**). Selective S-cone stimulation elicits no response in H1 cells (**e**). H2 cells respond (*right column*) to luminance modulation with a sustained hyperpolarization (**f**). There is no response to chromatic modulation (**g**). H2 cells hyperpolarize in response to L- and M-cone excitation (**h** and **i**) but also to S-cone excitation (**j**). Modified with permission from: Dacey et al. [45]

details of macaque bipolar cell classes were provided by a series of immunocytochemistry studies [38, 39, 41, 71, 73]. More recently, another series of studies revealed that marmosets and other New World monkeys with abovementioned polymorphic color vision possess the same classes of bipolar cells as macaques, indicating that color processing in bipolar cells is not based on its morphology [70, 72, 74, 75]. However, there is evidence that the cone inputs to centers and

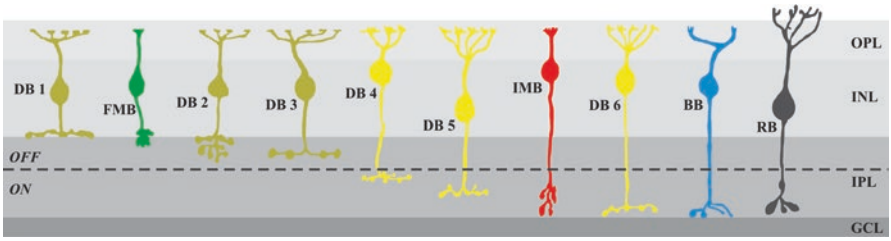


**Fig. 2.5** Schematic diagram of bipolar cell classes found in the primate retina. Cells were studied in retinal flat mounts or in transverse sections impregnated with the method of Golgi [35]. They were classified using morphological criteria: shape of dendritic trees, number of dendritic clusters, cell body position in the inner nuclear layer, shape and position of their axon terminals in the inner plexiform layer. *OPL* outer plexiform layer, *INL* inner nuclear layer, *IPL* inner plexiform layer, *GCL* ganglion cell layer, *OFF* superficial strata of the inner plexiform layer where the axon terminals of OFF bipolar cells branch, *ON* deep strata of the inner plexiform layer where the axon terminals of ON bipolar cells branch. Modified with permission from Boycott and Wässle [35]

surrounds of parvocellular retinal ganglion and LGN cells are more selective than expected on the basis of random wiring, indicating that in course of evolution the functional wiring of bipolar cells may have changed such that responses to color stimuli were increased [76] (see also Chap. 4). Below, we argue that electroretinograms (ERGs), that presumably reflect bipolar cell activity, can display responses that are reminiscent of those of the parvocellular pathway, suggesting that some bipolar cells (probably the midget bipolar cells) indeed may be involved in chromatic processing.

Bipolar cell classes comprise a single class of rod bipolar cells (RB cells) and at least nine different classes of cone bipolar cells: two midget bipolars (FMB cells and IMB cells), six diffuse bipolars (DB1–6 cells), and a single class of S-cone bipolars (BB cells) [32] (Fig. 2.5). In addition, giant cone bipolar cells (GB cells) have been reported in several studies [33, 35, 48, 68, 77, 78].

Midget bipolar (MB) cells make very distinct connections and form the origin of the M/L cone opponent parvocellular pathway which is considered to be the basis for the red-green channel of color vision. They connect small patches of the photoreceptor mosaic with small dendritic trees of midget ganglion cells (also called parvocellular or PC ganglion cells) in the inner plexiform layer [35, 41]. In the central region, MB cells have a single primary dendrite and a single dendritic cluster that contact the pedicles of one L- or M-cone. Single-cone MB cells are found up to 45 deg of eccentricity, but at greater eccentricities there is an increasing proportion of MB cells that have two to four dendritic clusters each contacting a distinct cone [41]. MB cells comprise two separate populations with distinctive morphology and connectivity: FMB cells make flat synapses with cone pedicles and send axons to the upper half of the inner plexiform layer while IMB cells make invaginating synapses with cone pedicles and send axons to the lower half of the inner plexiform layer [35, 41, 66]. Every M or L cone pedicle contacts an FMB and an IMB cell [79]. Below, we discuss the functional implication of these morphological findings for red-green color vision and for recent ERG findings.

BB cells form a pathway dedicated to conveying information from S cones to specific ganglion cells and thus provide S cone input to S-/ML-cone opponent pathways. They are probably the basis for blue-yellow color vision. BB cells are easily identified by their long, smoothly curved dendrites which are horizontally oriented in the outer plexiform layer and contact between one and three cone pedicles. Double labeling of BB cells and S cones showed that their dendrites are clearly cone-selective and reach toward one or more S cones, making invaginating synapses with them. Their axon terminals are relatively large and stratify in the deeper stratum of the inner plexiform layer, close to the ganglion cell layer.

DB cells comprise several different classes, some of them providing M or L cone input to S-/ML-cone opponent pathways, for which they provide the "yellow" input of the blue-yellow color channel. DB cells can be divided into two groups using similar criteria of flat and invaginating synapses as used for distinguishing MB cells: DB1, DB2, and DB3 make flat synapses with cone pedicles and send axons to the upper half of the inner plexiform layer while DB4, DB5, and DB6 cells make invaginating or flat synapses with cone pedicles and send axons to the lower half of the inner plexiform layer; the different classes have been sequentially numbered following the depth of their axon terminals in the inner plexiform layer [35, 38, 71]. A subdivision of DB3 cells into DB3a and DB3b has recently been proposed [72, 80, 81]. DB cells contact all cones in their dendritic trees by the means of multiple dendritic clusters (4–10 clusters in the retinal periphery) [35, 38, 71, 73, 82, 83], but DB4 and DB6 are biased against S cones and make proportionally more dendritic contacts with M and L cones [84] while there is no evidence for a bias in favor or against S cones in the other DB classes [82].

### *2.3.3 The Transmission of Photoreceptor Signals to Bipolar Cells*

Photoreceptor signals are transmitted to a series of post-receptoral elements that are described in the previous section which process these signals and send them to second order retinal neurons. The result is coded in the train of neural impulses sent by about 1,100,000 retinal ganglion cell axons to higher visual centers of the human visual system (described in Chap. 4). There are important limits to vision imposed by the properties of photoreceptors and post-receptoral neurons and, consequently, several aspects of the information content present in the retinal image are considerably transformed by retinal neural circuits. The existence of ON and OFF pathways, the temporal responses of different class of neurons, the spatial pooling by retinal elements of the same class, and the coding of spectral reflectance are relevant aspects of visual information processing that take place in the retina. In this section we describe those more directly relevant for color vision.

Cones and rods transmit their signals directly to horizontal cells and bipolar cells through complex synapses located at their axon terminals—cone pedicles and rod spherules, respectively. Cones of all classes and rods respond to light with changes of electrical potential across their plasma membrane, always with the same polarity.

When the light level is increased, cones and rods hyperpolarize and decrease the amount of glutamate released by the cone pedicles or rod spherules and, conversely, when the light level is decreased, cones and rods depolarize and increase the amount of glutamate released by their axon terminals. However, in the subsequent steps of the visual pathway there are not only neurons that respond to light in the same manner as photoreceptors, but also others that respond in the opposite way. Neurons that conserve the photoreceptor response polarity are called OFF cells while those that invert the photoreceptor response polarity are called ON cells [85, 86]. This is possible because there are complex mechanisms of photoreceptor signal transmission that conserve or invert the sign of photoreceptor responses to light based on different kinds of glutamate receptors that are found in the photoreceptor synapses [87]. Both classes of horizontal cells—H1 and H2 cells—and about half of the bipolar cell classes—DB1, FMB, DB2, DB3a, and DB3b cells, with axon terminals branching in the upper half of the inner plexiform layer—have AMPA and/or KA glutamate receptors (iGluRs) in their post-synaptic membranes facing the cones and rods axon terminals [88]. The ionotropic nature of these receptors means that they act directly by opening or closing ion pores in the plasma membrane, in this case responding to glutamate by increasing conductance to cations. A decrease of glutamate release by the photoreceptors in response to light results in a decrease of the iGluR activation and in a hyperpolarization of the post-receptoral horizontal and bipolar cells. These are consequently of the OFF type. The sign conserving synapses are located in horizontal cell dendrites (contacting cone pedicles) or axons (contacting rod spherules) that form the lateral elements of the triads in invaginating synapses. Flat synapses of cone pedicles with bipolar cell dendrites are also sign conserving [79]. Therefore, these bipolar cells are also of the OFF type. Their axon terminals are located in the outer half of the plexiform layer. BB and RB cells do not make flat synapse contacts with the S cones and rods, respectively, and they are exclusively of the ON-type.

DB4, DB5, IMB, DB6, BB, and RB bipolar cells, which have axon terminals progressively deeper in the inner half of the inner plexiform layer, have metabotropic receptors, i.e., they do not act directly via ion pores (although this can be the end effect of the cascade) but modify a G-protein molecule which in turn activates a secondary messenger molecule. These bipolars possess the glutamate receptor mGluR6 in their postsynaptic membranes [89]. The mGluR6 is a G-coupled receptor that activates a membrane phosphodiesterase, decreasing intracellular cGMP levels and, consequently, decreasing cGMP-dependent membrane conductance for cations. Thus, a decrease of glutamate release by the photoreceptors in response to increased light results in increased intracellular cGMP levels leading to an increased membrane cation conductance, which depolarizes the postsynaptic bipolar cells. Thus, these bipolar cells are ON cells and their dendrites constitute the central elements of the triads of the invaginating synapses with rod spherules or cone pedicles [79].

The retinal image is sampled at a spatial resolution that is initially determined by the photoreceptor mosaic. However, convergence of signals along the visual pathway may progressively degrade the spatial resolution. Convergence starts at the first synapses between photoreceptors and bipolar cells, and further increases in synapses between bipolar cells and ganglion cells. In macaque, convergence of

cones onto cone bipolar cells differs according to the bipolar cell class and varies only slightly as a function of retinal eccentricity: MB cells contact a single cone (1–4 in the retinal periphery), BB cells 1–3 cones, and DB cells 4–10 cones (with slight differences for different DB classes) [35, 39, 41]. The one-to-one connectivity between cones, MB cells, and PC-ganglion cells is preserved in the foveal region, but the convergence of MB cells onto PC-ganglion cells increases steeply with increasing retinal eccentricity [41]. In other visual channels, such as the one formed by cones connected to DB cells and thence to magnocellular (MC-) ganglion cells, the convergence of DB cells onto MC-ganglion cells also increases towards retinal periphery. Thus, the spatial resolution of PC-, MC-, and KC-(koniocellular) channels is set by their respective ganglion cell mosaics.

The ON/OFF dichotomy of bipolar cells and the convergence of single cones onto MB bipolar cells have important consequences for the M/L cone opponent mechanism of color vision. They result in the existence of four kinds of MB cells [32]. Two of these receive sign conserving synapses from a single M or L cone. These are the M-OFF FMB and L-OFF FMB cells. A further two receive sign inverting synapses from a single M or L cone. These are the M-ON IMB and L-ON IMB cells. In the central retina, each MB bipolar cell makes synapses with a single PC ganglion cell. Thus, PC ganglion cells have center-surround receptive fields with four different mechanisms driving the receptive field center, provided by the MB cells described above, and receptive field surrounds of opposite polarity whose origin is not well understood: M-OFF/L-ON, L-OFF/M-ON, M-ON/L-OFF, and L-ON/M-OFF cells. It is believed that these four ganglion cell subclasses underpin red-green color vision (reviewed in Chap. 4).

### *2.3.4 Midget, Parasol and Bi-stratified Ganglion Cells*

There are three major retinal pathways that process cone signals for conscious visual perception including color vision. The magnocellular (MC-) pathway consists of diffuse bipolar cells and parasol ganglion cells that project to the two ventral layers of the lateral geniculate nucleus (LGN). MC-ganglion cells receive additive input from the L- and M-cones, which makes them luminance sensitive. They are therefore the physiological basis of luminance vision [62, 63, 90–92] (see Chap. 4). They can respond to high temporal frequencies and have relatively large receptive fields and this is probably why their responses are used for motion processing [93]. Their large receptive fields make them probably less important for form perception, although their high responsivity for luminance stimuli allows them to code for spatial position on a hyperacuity level [94–96]. The receptive fields can be subdivided in centers and surrounds which are antagonistic. As described above for bipolar cells, stimuli leading to a luminance increase in the center (or a luminance decrease in the surround) lead to a depolarization in the ON-center cells and to a hyperpolarization in the OFF-center cells. Conversely, ON-center cells are hyperpolarized by luminance decreases in the centers and luminance increases in the surrounds. These stimuli lead to depolarizations in the OFF-center cells.

The PC-pathway contains midget bipolar cells and midget ganglion cells, which project to the four dorsal layers of the LGN. Like the MC-pathway, the PC-pathway processes exclusively L- and M-cone signals. However, in contrast to the MC-pathway, the cone signals provide opponent inputs. Furthermore, there are strong indications that the cone strengths are much more balanced compared to the MC-pathway, since the ratio of L-cone to M-cone responses in the parvocellular pathway is close to unity [97]. Again they have receptive fields with centers and surrounds. Foveal parvocellular cells have centers that receive input from only one cone. It is not clear yet if the surrounds receive inputs from the two cone types or whether there is a bias towards the cone type that is not represented in the center [98, 99]. With a random cone input, cone opponency would only occur because of the obligatory cone selective center. It is not clear in that case how an L:M cone ratio of about unity can arise. The centers of peripheral PC-cells are larger and again may receive mixed cone input (see above). However, under such circumstances the cells would lose their cone opponency.

Again there are ON- and OFF-center cells so that in the end there are four types of parvocellular ganglion cells (+L−M, +M−L as the ON-center cells; OFF-center cells are −L+M and −M+L) The L-/M-cone opponency in the parvocellular ganglion cells is the physiological basis for red-green color vision. The small receptive field sizes are probably used for the perception of forms of objects [100, 101].

The KC-pathway processes input from all three cone types, in which the S-cone signals are antagonistic to those from L- and M-cones (i.e., the cone input can be described as +S-[L+M]). As described above, two types of bipolar cells are involved: DB cells provide the L- and M-cone inhibitory signals whereas the S-cone excitatory signal are transmitted by BB cells [102]. The ganglion cells belonging to this pathway are of the small-field bi-stratified type [44] and project to the interlaminar regions and the areas surrounding the parvocellular and magnocellular layers of the LGN. The antagonistic input is not organized in center and surround substructures of the receptive fields; instead they are spatially co-extensive and constitute Hubel and Wiesel's [103] type 2 cells. Therefore these cells are thought to be unimportant for spatial vision but provide the basis for blue-yellow color vision.

The physiological properties of retinal ganglion cells and neurons in the LGN are well described. Those of primate bipolar cells are less well known. From recent ERG data, it can be inferred that the properties of the diffuse and midget bipolar cells are very similar to those of the MC- and PC-ganglion cells respectively (see below).

## 2.4 Photoreceptor and Post-receptoral Processes Leading to the Electroretinogram

The electroretinogram (ERG) is an electrical signal of retinal origin that is elicited by the same excitation of photopigments that leads to a visual response. The ERG has important clinical value because it is a non-invasive electrophysiological, and thus objective, method which can be used to monitor the functional integrity of the

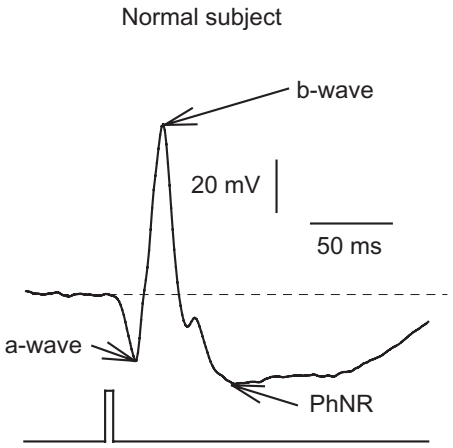


**Fig. 2.6** Example of a full field flash ERG measured in a normal subject. The main components are identified

retina. In addition, the ERG has emerged as an important tool for the measurement of retinal function in animals in vivo. This has been particularly evident following the development of transgenic mouse lines, where the retinal organization has been genetically altered, and the use of mouse models of retinal diseases.

Originally, the ERG was measured to short light pulses [104]. These flash ERGs are still measured. However, increasing numbers of other stimuli and resulting ERG types are measured nowadays. Below, we describe those that are important for revealing cone opponent processes. In the flash ERG, three components can be distinguished that have different cellular origins (Fig. 2.6). The early negative a-wave originates in activity of the photoreceptors and off-bipolar cells The next wave is positive b-wave that is mainly determined by activity of on-bipolar cell [105]. The b-wave of the flash ERG is in fact an addition of a positivity as a response to stimulus onset and a slightly delayed positive response to stimulus offset known as the d-wave [106]. The d-wave has identical implicit times to stimulus offset as the a-wave after stimulus onset indicating that they have the same cellular origins [107]. The b-wave is followed by a photopic negative response (PhNR) that reflects activity of retinal ganglion cells [108–110].

The value of the ERG in studying vision, and more particularly color vision, is, however, not straightforward. Armington [111] in his book "The Electroretinogram" emphasized the potential of the ERG in the study of visual processing in the retina. Yet at the same time he was also aware of the difficulties in establishing correlations between the ERG and psychophysical data.

### *2.4.1 Early Research on Chromatic Processes in the ERG*

Armington [111] dedicated a whole chapter to the ERG related to human spectral sensitivity and color vision. As discussed above, different cone spectral sensitivities are necessary but not sufficient for color vision. Cone opponent processing is a

second prerequisite for color vision. At the time when Armington's book appeared, the notion of cone opponency was still quite novel [112]. Riggs and colleagues [113, 114] showed, using equiluminant alternating gratings (5.35 Hz; 10.7 reversals per second), that the wavelength separation for a criterion ERG response is similar to psychophysically derived measures of wavelength discrimination with minima around 500 and 600 nm, indicating that repetitive stimuli may elicit ERGs that reflect cone-opponent processing.

Beginning in the early 1970s, data on the spectral sensitivity of the b-wave in flash ERGs emerged [115–119]. The b-wave spectral sensitivity as a function of wavelength of flashed stimuli upon a background displayed similarities with psychophysically determined detection sensitivities using similar stimuli [118, 120]. Such spectral sensitivities are an indication that detection is mediated by cone opponent mechanisms. Nowadays, the b-wave is thought to originate from bipolar cell activity [121]. Armington [122] found spectral sensitivities that also indicated spectral opponent processing as early as 1959, but at that time the data were difficult to interpret. The similarity with the psychophysical data indicates that the same postreceptoral mechanisms may underlie the psychophysical and ERG data.

On the other hand, the a-wave exhibits different spectral sensitivity which does not reflect cone opponent processing, indicating that it has a different cellular origin. Indeed, it is now thought that the a-wave mainly reflects the activity of the photoreceptors and the OFF-bipolar cells. The main origin of the b-wave resides in the ON-bipolar cells [105].

Single cell recordings in the 1960s showed that retinal ganglion cells and LGN cells could display cone opponent processing [103, 123], indicating that the subtractive interaction between cone signals, necessary for color vision, occurs already in the retina. The exact site was, and still is, not exactly known. Data from fish and turtle indicated that cone opponency occurs in the outer retina in these species and Baron [124] proposed that, similarly, opponency might also occur there in primate and would therefore be discernable in the primate ERG. He described a component that possibly reflects cone opponency in the foveal ERG of monkeys using intraretinal electrodes. This component could subsequently also be identified in the ERG as measured at the cornea [125]. However, the data are not easy to interpret as being related to cone opponency. Nowadays it is clear that cone opponent processing in "lower" vertebrates and in primates is quite different. Horizontal cells in turtle and fish retinae show distinct cone opponency [65] that is absent in horizontal cells of the primate [45].

### *2.4.2 Recent Developments*

One possible reason for the limited correlation between early ERG and psychophysical data is that ERGs were mainly measured to short flashes of light. Possibly, the circuitries leading to an ERG and those leading to a visual percept have substantially different response properties when using very short stimuli. In the following

section, we provide evidence that the use of repetitive stimuli, leading to steady state responses, may reveal more similarities between ERG and psychophysical data. One example of the use of repetitive stimuli is the heterochromatic flicker photometry (HFP) method that is also used in psychophysical measurements to determine the luminance of a light source. Briefly, two lights, a reference and a test light, are modulated in counter-phase at relatively high temporal frequencies ($\geq$16 Hz) at equal and fixed contrast. The mean luminance of the test light is altered by the subject to minimize the perception of flicker, where, by definition, the two lights are equiluminant. Using the same stimuli, it proved to be possible to also minimize the ERG response. The spectral sensitivities that could be measured in this way were also identical in psychophysical and ERG experiments (resulting into the photopic spectral luminosity function, $V_\lambda$ [126–131]). Furthermore, the HFP method leads to psychophysical results that differ between different individuals. This inter-individual variability was also present in the ERG data [129] and is the result of a variability in the ratio of L- to M-cone signals in the luminance channel. The L/M cone ratio could also be measured directly in psychophysical and ERG experiments and it was shown that the amplitude ratio of the high frequency ERG in response to L- and M-cone isolating stimuli can be correlated to the sensitivity ratio for detection of L- and M-cone isolating at high temporal frequencies [132, 133]. At high temporal frequencies, the ratio is on average about 2:1 and reflects the ratio of L- to M-cone packing densities [134]. Data from RNA expression have shown that the far peripheral retina may contain nearly exclusively L-cones [135–137]. This peripheral L-cone dominance was also found with ERG measurements [138, 139]. Finally, changes in L/M cone sensitivity ratio in individual observers, caused by difference states of adaptation, were again also represented in the L/M cone amplitude ratio in the high temporal frequency ERG [28].

The correlations described above between psychophysics and ERGs were found for high temporal frequency stimuli (about 25 Hz and higher) where the psychophysical data were mediated by the luminance channel of which the MC-pathway is the physiological basis. The question is: are there also ERG responses to modulating stimuli that can be linked to chromatic sensitivities? Psychophysically, chromatic sensitivity can be mainly measured at lower temporal frequencies [92, 97, 140, 141]. If stimuli contain both luminance and chromatic modulation, then psychophysical detection thresholds are mediated by the chromatic channel at low temporal frequencies and by the luminance channel at high temporal frequencies [92, 141]. With L- and M-cone isolating stimuli, chromaticity and luminance are simultaneously modulated and detection thresholds for these stimuli are indeed determined by the luminance content at high temporal frequencies and by the chromatic modulation at low temporal frequencies [132].

Recently, it has indeed been found that the ERG responses to intermediate temporal frequency stimuli (around 12 Hz), containing red-green chromatic contrast, can reflect activity of the L-M opponent parvocellular pathway. The evidence for this comes from several experiments. In the first type of experiment, L- and M-cone isolating stimuli are used (see Fig. 2.7). L- and M-cone driven responses are of about equal amplitudes and thus the L:M ratio is close to unity at intermediate temporal frequencies (about

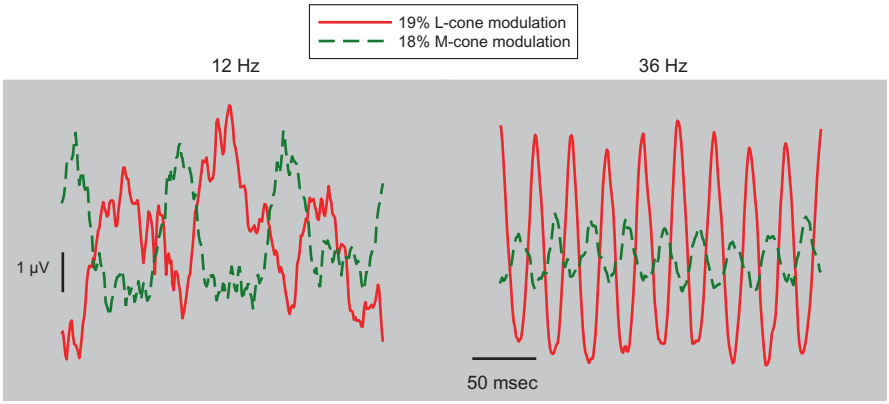


**Fig. 2.7** ERG responses in a trichromatic subject to full field L- and M-cone isolating stimuli of similar contrast (18 % M-cone contrast: *dashed green line*; 19 % L-cone contrast: *solid red line*) at two temporal frequencies: 12 Hz (*left*) and 36 Hz (*right*). Triple silent substitution conditions were used (i.e., only the photoreceptor type of interest—either L- or M-cones—were stimulated; the three others were silenced). The 12 Hz responses have similar amplitudes whereas the L-cone driven responses are larger than the M-cone driven responses at 36 Hz [143, 144]

12 Hz). At high temporal frequencies (30 Hz and above), the L-cone driven responses are larger than the responses to M-cone isolating stimuli [142–144]. Furthermore, the phases of the L- and M-cone driven responses can behave differently at low and high temporal frequencies. Generally, the phases of the response to L- and M-cone isolating stimuli at intermediate temporal frequencies are about 180° apart indicating cone opponency. The phase differences at high temporal frequencies seem to be more variable. They can be large as well (as is seen in Fig. 2.7) but there are conditions in which the phase of L- and M-cone driven responses are relatively similar [26].

In the second type of experiment, red and green lights were modulated sinusoidally in counter-phase. The contrasts of the two were varied such that the sum of the red and green contrasts (R + G) was kept constant. Thus, the fraction of red contrast relative to the total contrast (R/(R + G)) was varied (and the fraction of green contrast was complementary; see Fig. 2.8a). The chromatic contrast (Fig. 2.8b left plot; red line) in these stimuli was constant. The luminance contrast (Fig. 2.8b left plot; black line), however, varies linearly as a function of red fraction, reaching zero when R/(R + G) is about 0.5 (depending on the present L:M ratio of the signals entering the luminance signal). Also, the phase has different characteristics (Fig. 2.8b right plot): the phase of the chromatic output is constant whereas the luminance modulation follows the modulation of the green light for small values of R/(R + G) and is determined by the red stimulus when R/(R + G) is larger than 0.5. Using this type of stimulus it was found that the responses to high frequency stimuli (Fig. 2.8c) were very similar to the expected activity of the luminance channel with a clear minimum [145]. In accordance with the notion that the responses reflect luminance activity, the phase changed by 180° at the amplitude minimum. These data are in accordance with the well-known flicker photometric data, described

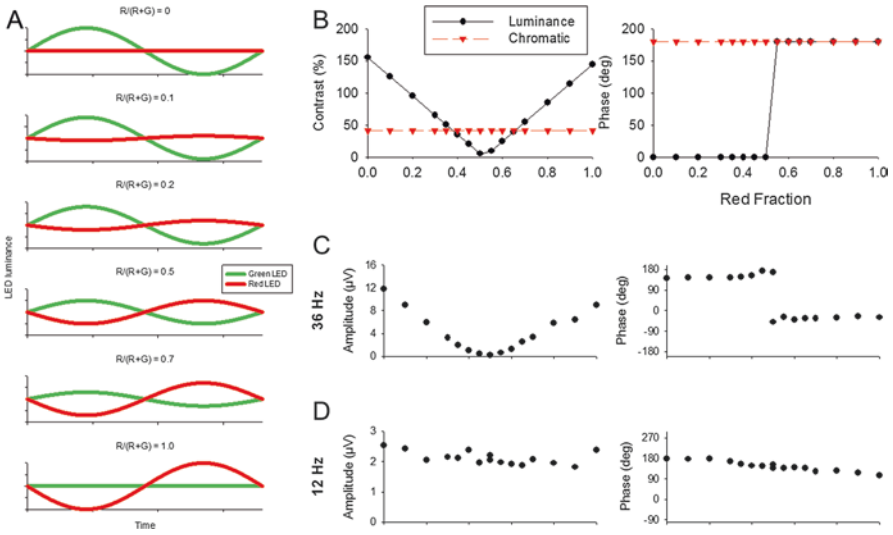


**Fig. 2.8** Results of ERG experiments with red-green sinusoidal modulation. (**a**) Six examples of stimuli. One period is shown. The red and green lights (from light emitting diodes; LEDs) were modulated sinusoidally in counterphase. The mean luminance levels were equal for the red and green lights and were not varied. The contrast in the two lights was varied, but the sum of the *red* and *green* contrast was constant. (**b**) Expected output amplitude (*left plots*) and phase (*right plot*) of the luminance channel (*black line*) and red-green chromatic channel (*red line*) as a function of red fraction in the stimulus. (**c**) ERG response amplitude and phase to 36 Hz stimuli as a function of red fraction. Observe the resemblance with the expected response of the luminance channel in **b**. (**d**) Response characteristics measured in the same observer at 12 Hz. These responses are like those of the red-green chromatic channel in **b** (Adapted from Kremers et al. [145].)

above. More importantly, it was found that at an intermediate temporal frequency (12 Hz) neither amplitude nor phase changed appreciably as a function of red fraction (Fig. 2.8d), thereby resembling the properties of the red-green chromatic channel.

An important control experiment was performed with dichromats, who lack a functional red-green chromatic channel because they only possess L or M cones. In these subjects, the responses at all temporal frequencies clearly followed the response properties of the sole cone type (Fig. 2.9), indicating that the mechanism that is responsible for the ERG responses at 12 Hz, is not present in the dichromats, and thus most probably originates in the red-green chromatic channel.

In the third type of experiment, red and green lights were again modulated in counter-phase. But now they were alternately activated. That means that when one light is switched on the other is switched off and vice versa. When activated, the output of the light sources followed a raised cosinusoidal profile. The luminance output of the red and green light were carefully balanced to be equal in luminance. As a result, the chromaticity of the stimulus is modulated at a temporal frequency that is half the luminance frequency (see Fig. 2.10). In this experiment, the temporal frequency of the stimulus was varied. In contrast to the second experiment, where the LEDs were

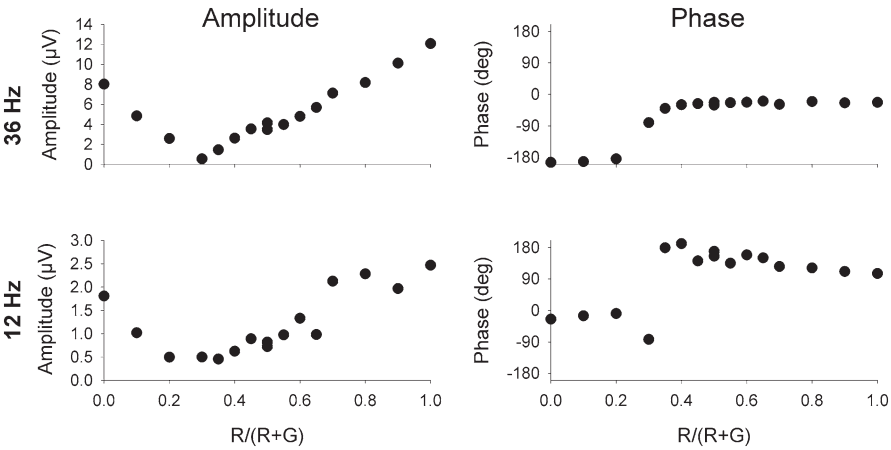


**Fig. 2.9** Responses measured in a deuteranope. The same stimuli as displayed in Fig. 2.8 were used. Both the 36 Hz (*upper plots*) and 12 Hz (*lower plots*) responses display the characteristics of a luminance reflecting mechanism. The minimum has shifted towards smaller values of the red fraction in the stimulus. This can be expected for responses that are exclusively driven by L-cones. (Adapted from Kremers et al. [145])

always simultaneously activated, here only one LED is activated at a time. Furthermore, in this experiment the luminance was always modulated with 100 % contrast, whereas the luminance modulation in the second experiment was variable and did not exceed 50 % (for the conditions in which R/(R + G) were 0 and 1). In single cell recordings from the macaque retina it was found that the PC-ganglion cells mainly responded at the frequency of the chromatic modulation whereas MC-cells mainly responded to the luminance modulation (i.e., at twice the response frequency of the parvocellular cells; [146]). These stimuli were also used while recording the ERGs (Fig. 2.10, upper plots). In these experiments, it was found that the high temporal frequency ERGs of normal trichromats (Fig. 2.10, left two columns) contained, almost exclusively, frequency components that were identical to those of the luminance modulation in the stimulus. No response was observed at the chromatic modulation frequency. At low and intermediate temporal frequencies, a clear response component at the frequency of the chromatic modulation was present. In Fig. 2.10, this can be observed because the responses to the red and green stimuli are dissimilar at low temporal frequencies (here particularly for the 6 Hz stimulus conditions). The latter component could not be observed in red-green dichromats (Fig. 2.10, the two right columns) because the responses to the red and green stimuli were very similar in the dichromats also at low temporal frequencies. This result strongly indicates that this component indeed originates in the red-green chromatic channel [147].

In a fourth experiment, transient ERG responses to L- and M-cone isolating stimuli with sawtooth and square-wave temporal profiles were measured [148, 149]. With sawtooth and square wave stimuli, On- and Off-responses (i.e., responses to sudden increments or decrements in cone excitation) can be studied separately. These measurements revealed a response inversion: responses to L-increments

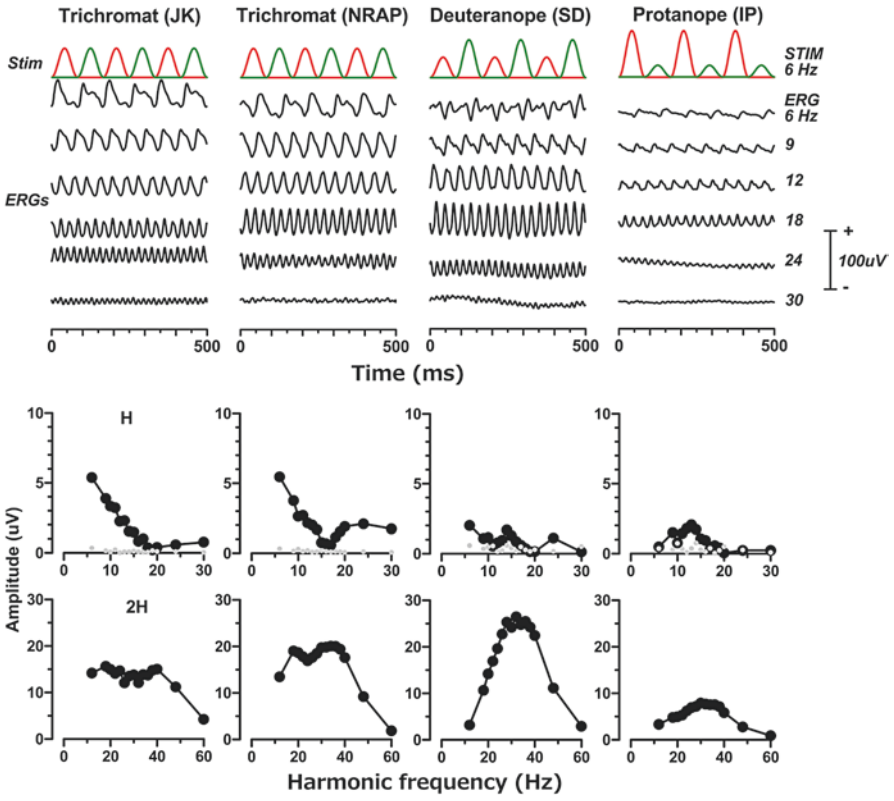


**Fig. 2.10** Results of ERG recordings performed with alternating red and green stimuli. *Top rows*: Depiction of the stimuli with Raw ERG responses. In the *left two columns*, recordings in trichromats are displayed, whereas the *right two columns* show the responses measured in dichromats (a deuteranope and a protanope). The temporal frequencies, given on the *right*, indicate the frequency of the luminance modulation in the stimulus. The temporal frequency of the chromatic modulation equals half the luminance frequency. *Two bottom rows*: Amplitude as a function of temporal frequency of the first (chromatic) and second (achromatic) harmonics. Note the marked reduction in the chromatic response in the dichromats, particularly at low temporal frequencies. Adapted from Parry et al. [147]

(L-On) resembled those to M-decrements (M-Off) and the responses to L-decrements (L-Off) and M-increments (M-On) were similar in waveform (see Fig. 2.11 for responses to sawtooth stimuli). The responses to L-cone isolating stimuli had the same polarity as the responses to luminance modulation with the same temporal profile [148, 149]. The response inversion between L- and M-cone driven responses suggests that cone opponent processes are involved. Furthermore, the data show that the textbook explanation of the origins of the different components [105], in which only On- and Off-bipolar cells without a distinction between the responses from for example midget and diffuse bipolar cells, is probably only part of the story. The data strongly suggest that such a distinction between different types of midget bipolar cells should be taken into account. Although the response inversion seems to be

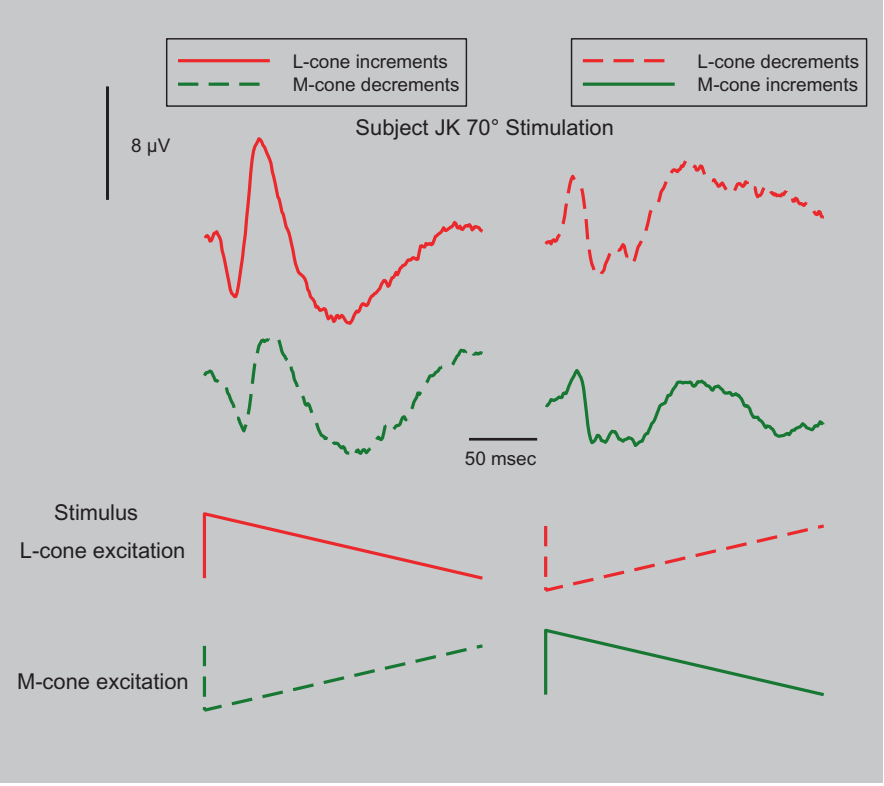


**Fig. 2.11** Responses to L- and M-cone isolating sawtooth stimuli (4 Hz temporal frequency). The *left column* displays the responses to L-cone increment stimuli (*solid red line*; the L-cone excitation is rapidly increased and gradually decreased as shown in the stimulus sketch below) and to M-cone decrements (having the opposite profile; *dashed green line*). The *right column* shows the responses to L-cone decrements (*dashed red line*) and M-cone increments (*solid green line*). Observe that the responses to L- and M-cone isolating stimuli of opposite polarities resemble each other [148]. This effect was also found in responses to square wave stimuli [149] but may be less clear for full field stimuli [148]

present for all response components (a-, b-, d-wave-like and other components), the picture is more complicated because the ratios of the L- and M-cone signal strengths is different for the different components. The early components (a- and d-wave) display large L:M ratios and resemble the ratios of cone numbers and of the psychophysical luminance channel. The later components (b-wave and photopic negative response) display an L/M ratio closer to unity, suggesting stronger chromatic input [148]. The responses to M- and L-cone increments in protanopes and deuteranopes respectively had similar waveforms indicating that the inversion of responses is not present in dichromats [148, 149].

From these experiments, a picture emerges that, in trichromatic observers, ERG responses to stimuli that contain luminance and red-green chromatic modulation reflect activity of the luminance channel and the MC-pathway at high temporal frequencies (≥30 Hz). This is also the basis of the ERG results with the HFP paradigm.

At intermediate temporal frequencies (between about 8 and 14 Hz), the ERG reflects the activity of the red-green chromatic channel and of the PC-pathway. Therefore in the years since Armington's book appeared, evidence has been obtained in favor of the notion that ERG signals indeed can reflect the properties of post-receptoral retinal pathways and have perceptual relevance. This result may be of importance for basic vision research because it now will be possible to study properties of these pathways and channels in human subjects using objective non-invasive techniques.

To investigate the influence of the size and spatial configuration of the stimulus on the two pathways, ERGs were recorded using L- and M-cone isolating sinusoidal stimuli at intermediate (8 and 12 Hz) and at high (30, 36, 42, and 48 Hz) temporal frequencies. These responses were measured for full field stimuli and for circular stimuli with different diameters. In addition, annular stimuli with different inner diameters were used [139]. The response amplitudes at high temporal frequencies strongly depended on stimulus area. The responses to 8 and 12 Hz stimuli were similar for all stimulus areas except for the smallest circular stimulus. The responses at high temporal frequencies increase with increasing stimulus size (Fig. 2.12). This

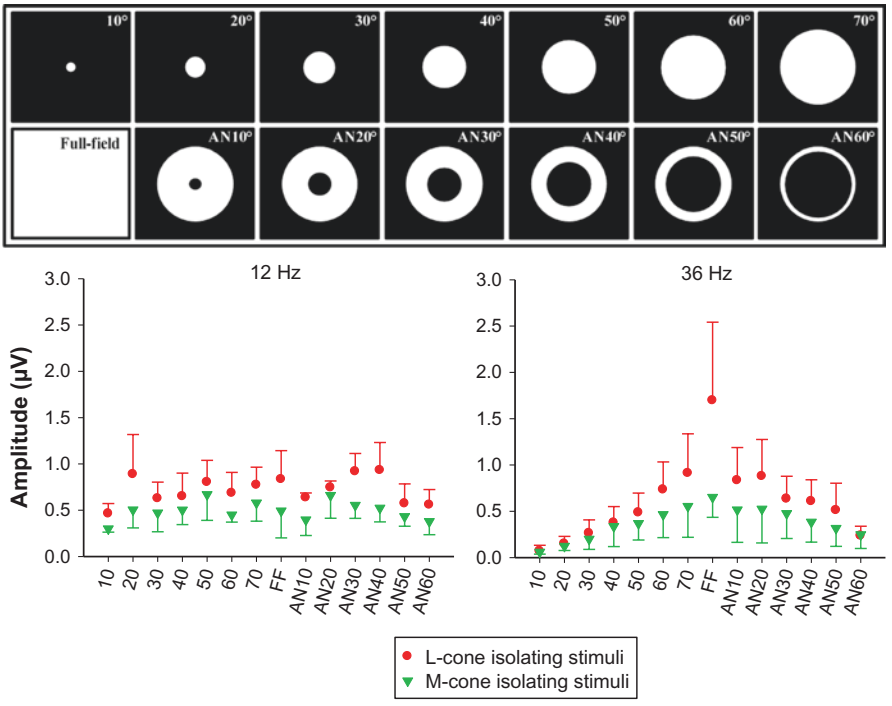


**Fig. 2.12** Response amplitudes to sinusoidal modulation of L- and M-cone excitation for different stimulus spatial configurations. Responses at two different temporal frequencies (*left plot*: 12 Hz; *right plot*: 36 Hz) are shown. The sketch above the plots shows the spatial stimulus configurations that were used and corresponds to the labels on the *x*-axes of the plots. Amplitude does not vary strongly with spatial configuration at 12 Hz. The 36 Hz stimuli strongly depend on the spatial arrangement of the stimuli. Redrawn from Ref. [139]

indicates that the PC- and MC pathways may either have different spatial distributions or their response characteristics change differently with retinal eccentricity.

The physiological properties of retinal ganglion cells and neurons in the LGN are well described (see above and Chap. 4). Those of primate bipolar cells are less well known. ERG responses to repetitive stimuli mainly reflect activity of bipolar cells [121]. From the results of the ERG measurements, it can be inferred that the properties of the diffuse and midget bipolar cells are probably very similar to those of the MC- and PC-ganglion cells respectively, indicating that these properties are already present after the first synapse (from photoreceptors to bipolar cells) in the visual pathway. Sperling and colleagues' work, showing that the b-wave may also reflect cone opponent processing [115–118], is in agreement with this proposal because the b-wave is also thought to originate in bipolar cell activity [105]. It should be noted, however, that bipolar cells not only receive feed forward signals from photoreceptors but also from horizontal cells. They also receive feedback signals from horizontal and amacrine cells. These signals influence their response properties. Furthermore, KC-cell responses make use of two types of bipolar cells, one of which (the diffuse bipolar cell) has properties similar to that of the magnocellular channel. Therefore it is possible that the bipolar cells belonging to the +S-(L+M) pathway do not display similar physiological properties as the small field bi-stratified cells. Combined with the fact that S-cones and KC+S-(L+M) ganglion cells are much sparser than the other cone and ganglion cell types, respectively, possibly make the signals of this pathway in the ERG difficult to detect.

## 2.5 Open Questions

These new developments open up many possibilities to answer basic scientific and clinical questions. However, some important issues arise from this work and in the following section we give an overview of the key questions that we have identified.

### *2.5.1 How Can a Chromatic ERG Signal Appear at all with Four PC-Cell Types?*

ERG responses may reflect photoreceptor activity because all photoreceptor types hyperpolarize. However, there are two types of luminance sensitive (DB) bipolar cells: the ON- and the OFF-DB cells. Thus, if one type is hyperpolarized the other will be depolarized and vice versa. Therefore it could be expected that the responses of the two cell groups may cancel each other out (particularly when the two populations contain similar cell numbers) and no luminance ERG would be measurable unless there are physiological differences between ON- and OFF-DB cells. That is indeed the case (such as the abovementioned differences in glutamate receptors). Thus, luminance ERG responses can perhaps be measured because of the physiological differences between ON and OFF DB cells.

Although the differences between ON- and OFF-bipolar cells may explain why a luminance-based ERG can be measured, the situation is more complicated for ERGs that might reflect bipolar cell activity belonging to the PC-pathway. Instead of two there are four cell types present: +L-M, -L+M, +M-L, and -M+L. Again there may be a difference between ON- (+L-M and +M-L) and OFF- (-L+M and -M+L) center cells. But to be able to record an ERG driven by these cells, another asymmetry must be present because the responses to for example the +L-M and the +M-L cells could be expected to cancel each other. One possibility is that the differences in L- and M-cone numbers may also lead to different numbers of cone opponent bipolar cells (so that subjects with a many more L-cones than M-cones also have many more +L-M than +M-L bipolar cells). That would indicate a correlation between that the amplitude of the cone opponent ERG response and the L:M ratio. Although this has never been directly studied, there are no indications that such a correlation exists.

### *2.5.2 What Are the Effects of Selective Adaptation?*

We have observed that small cone-selective adaptations using a CRT screen may strongly influence the amplitudes of L- and M-cone driven ERG responses, resulting in a dramatic change in the L:M ratio. This is paralleled by a similar change in the psychophysical L/M sensitivity ratio [28]. However, Jacob et al. showed that even large changes in state of adaptation do not have a dramatic influence on ERG responses [139]. The latter results were obtained with a four primary LED stimulator. In contrast to this LED stimulator, complete isolation is not possible when a trichromatic observer views a CRT screen. However, it is improbable that the type of stimulator influences the results dramatically [150]. Furthermore, control experiments with the CRT screen showed that rod driven responses probably have little influence on the results. In conclusion, it seems that adaptation can influence ERG and psychophysical results dramatically, but it has not been possible to systematically describe this influence, let alone understand the underlying mechanisms. The fact that the effects of adaptation were also found in psychophysical experiments shows that answering this question may be very important for a better understanding of retinal adaptation processes.

### *2.5.3 Are There Fundamental Differences Between Protanopes and Deuteranopes?*

During the course of several years of studying deuteranopes and protanopes with ERG and psychophysical techniques, some important differences have been revealed. L-cone isolated stimuli normally do not lead to measurable ERG

responses in protanopes but M-cone isolating stimuli elicit small but measurable ERGs in deuteranopes [28, 143, 144, 148, 149]. In addition, in psychophysical experiments, protanopes cannot detect L-cone isolating responses even at the highest possible contrast, whereas M-cone isolating stimuli can often be detected by deuteranopes (although the threshold contrasts are substantially higher than for L-cone isolating stimuli [28]). In addition, adapting the L-cones has no effect on the ERG responses and psychophysical thresholds in protanopes. In deuteranopes, M-cone adaptation has effects that are similar to those of trichromats [28]. From control experiments, it was inferred that these differences cannot be caused by rod stimulation and adaptation that were not controlled with the stimuli displayed on a CRT screen. Deuteranopes often display larger responses than protanopes (see the responses of the dichromats displayed in Fig. 2.10), an observation that cannot be explained by differences in L- and M-cone contrast in the stimuli. Finally, as described in Chap. 10 a substantially larger number of deuteranopes pass color vision tests in comparison to protanopes.

The differences between deuteranopes and protanopes were found systematically in several experiments. The cause of these differences is still unclear. One possibility may lie in the fact that that on the X-chromosome there is normally only one copy of the L-opsin gene but that multiple copies of the M-opsin gene may be present [151]. Thus, if the first copy is defective, the subject might be diagnosed to be a deuteranope. If the downstream copies are normal they might lead to a residual activity of M-opsin. However we found no relation between the number of M-opsin genes and the magnitude of residual M-opsin activity [28] although more detailed analyses might be needed. Another explanation might be that an additional pigment might be involved. If the residual responses were present with M-cone stimuli and not with L-cone stimuli it can be expected that this pigment mainly absorbs shorter wavelengths. It is attractive to speculate that melanopsin-driven responses, present in the internally photoreceptive retinal ganglion cells (ipRGCs) may lead to measurable ERG responses and psychophysical flicker detection. Finally, small errors in the assumed density of the macular pigment and variability in photopigment absorption spectra may lead to particularly large for M-cone isolating conditions (that should be abolished in the deuteranopes) in comparison with L-cone isolating stimuli (that should not elicit responses in protanopes). Recently, a simulation of the effects of this variability has indeed shown that variability in L-cone fundamentals may lead to small L-cone stimulations in intended M-cone isolating stimuli. Although the L-cone stimuli are small they may be detectable in the absence of other responses. The residual stimulation of M-cones in L-cone isolating conditions is much smaller (Huchzermeyer and Kremers, Journal of the Optical Society of America A, Accepted for publication). The first two possibilities are highly speculative, the third explanation needs less assumptions. Remains, that there are systematic differences between deuteranopes and protanopes that are very conspicuous.

### 2.5.4 *How Can the Intermediate Temporal Frequency (8–16 Hz) ERG Have Very Similar Response Amplitudes for a Large Range of Different Spatial Configurations of a Stimulus?*

It was found that the ERG responses to intermediate temporal frequencies (reflecting activity of the PC-pathway) are relatively similar for different sizes of circular and annular stimuli (see Fig. 2.12) [139]. If this were the case only for circular stimuli, the results could be explained by the possibility that the pathway leading to the ERG responses would be mainly located at the central retina (up to about 10 deg eccentricity). However, the response amplitudes were often very similar with annular stimuli, in which this central area is not stimulated. A possible explanation is that the responses may summate over a retinal area up to a maximum at which it then saturates so that further increase of stimulus area has no effect. Signal processing would be similar at different retinal eccentricities, indicating that the retina would be relatively homogeneous up to an eccentricity of at least 35 deg. This is a surprising idea that certainly needs further experimental testing.

## 2.6 Future Perspectives

The recently reported correlations between ERG and psychophysical data give rise to the likelihood that the ERG may experience a renaissance in studies of human retinal processes that are relevant for visual perception. Furthermore, the correlation between ERG data and the physiology of the two main retino-geniculate (PC- and MC-) pathways suggests that properties of these pathways can now be studied directly in human observers using electrophysiological techniques. This also opens perspectives for understanding retinal mechanisms underlying color vision.

The abovementioned questions are waiting to be investigated. Answers to them will provide important information about color processing. Cone selective adaptation may for instance shed light upon adaptation mechanisms in the PC-pathway that may then be compared to adaptation mechanisms in the MC-pathway. If the differences between deuteranopes and protanopes are confirmed then this may point at fundamental differences in L- and M-cone driven responses and novel fundamental properties of retinal physiology may become apparent.

Developments in ERG recording techniques may not only have influence on basic visual neuroscience but also on clinical vision science and ophthalmology. The ERG has the potential to allow for better diagnoses of retinal disorders and for clearer identification of their cellular origins. If a disease primarily affects a particular photoreceptor type (as AMD is thought to initially affect the rods) or a particular cell circuitry (as glaucoma was for some time thought to lead to defects mainly in

MC-ganglion cells) then we can expect that ERG recordings that assay the responses of these cell types may be suitable for sensitive disease diagnosis. These techniques may also give an indication about how vision can be affected by disease processes and importantly, may allow the investigation as to how therapeutic interventions can affect visual performance in patients.

Of course other technical developments may bring a huge increase in our understanding of cone opponency and color processing in the primate retina. Recordings with multi-electrode arrays will bring a huge amount of new data. Furthermore, they may provide information about response interactions between different types of retinal neurons. The emerging field of optogenetics also has the potential to allow studying the retina and its constituent neurons in a very precise manner. Using optical techniques, the production of certain proteins can be manipulated and their function then be studied. These developments are extremely exciting and we expect them to bring completely new insights.

**Acknowledgements** Luiz Carlos da Silva Silveira passed away on 10th July 2016. This work was supported by German Research Council (DFG) grants KR 1317/9-1, KR1317/9-2 and KR1317/13-1.

## References

1. Berson DM, Dunn FA, Takao M. Phototransduction by retinal ganglion cells that set the circadian clock. Science. 2002;295(5557):1070–3. doi:10.1126/science.1067262.
2. Hattar S, Liao HW, Takao M, Berson DM, Yau KW. Melanopsin-containing retinal ganglion cells: architecture, projections, and intrinsic photosensitivity. Science. 2002;295(5557):1065–70. doi:10.1126/science.1069609.
3. Dacey DM, Liao HW, Peterson BB, Robinson FR, Smith VC, Pokorny J, et al. Melanopsin-expressing ganglion cells in primate retina signal colour and irradiance and project to the LGN. Nature. 2005;433(7027):749–54. doi:10.1038/nature03387.
4. Brown TM, Gias C, Hatori M, Keding SR, Semo M, Coffey PJ, et al. Melanopsin contributions to irradiance coding in the thalamo-cortical visual system. PLoS Biol. 2010;8(12):e1000558. doi:10.1371/journal.pbio.1000558.
5. Lall GS, Revell VL, Momiji H, Al Enezi J, Altimus CM, Guler AD, et al. Distinct contributions of rod, cone, and melanopsin photoreceptors to encoding irradiance. Neuron. 2010;66(3):417–28. doi:10.1016/j.neuron.2010.04.037.
6. Allen AE, Storchi R, Martial FP, Petersen RS, Montemurro MA, Brown TM, et al. Melanopsin-driven light adaptation in mouse vision. Curr Biol. 2014;24(21):2481–90. doi:10.1016/j.cub.2014.09.015.
7. Ecker JL, Dumitrescu ON, Wong KY, Alam NM, Chen SK, LeGates T, et al. Melanopsin-expressing retinal ganglion-cell photoreceptors: cellular diversity and role in pattern vision. Neuron. 2010;67(1):49–60. doi:10.1016/j.neuron.2010.05.023.
8. Naka KI, Rushton WA. S-potentials from colour units in the retina of fish (Cyprinidae). J Physiol (London). 1966;185:536–55.
9. Smith VC, Pokorny J. Spectral sensitivity of the foveal cone photopigments between 400 and 500 nm. Vision Res. 1975;15:161–71.
10. DeMarco P, Pokorny J, Smith VC. Full-spectrum cone sensitivity functions for X-chromosome-linked anomalous trichromats. J Opt Soc Am A. 1992;9(9):1465–76.

11. Stockman A, MacLeod DIA, Johnson NE. Spectral sensitivities of the human cones. J Opt Soc Am A. 1993;10(12):2491–521.
12. Stockman A, Sharpe LT. Cone spectral sensitivities and color matching. In: Gegenfurtner K, Sharpe LT, editors. Color vision: from genes to perception. Cambridge: Cambridge University Press; 1999. p. 53–88.
13. Sharpe LT, Stockman A, Jägle H, Knau H, Klausen G, Reitner A, et al. Red, green and red-green hybrid pigments in the human retina: correlations between deduced protein sequences and psychophysically-measured spectral sensitivities. J Neurosci. 1998;18:10053–69.
14. Stockman A, Sharpe LT, Fach C. The spectral sensitivity of the human short-wavelength sensitive cones derived from thresholds and color matches. Vision Res. 1999;39(17): 2901–27.
15. Wyszecki G, Stiles W. Color science: concepts and methods, quantitative data and formulas. New York: Wiley; 1982.
16. Stiles WS. Increment thresholds and the mechanisms of colour vision. Doc Ophthalmol. 1949;3:138–63.
17. Stiles WS. Color vision: the approach through increment threshold sensitivity. Proc Natl Acad Sci U S A. 1959;45:100–14.
18. Donner KO, Rushton WAH. Retinal stimulation by light substitution. J Physiol. 1959;149:288–302.
19. Estévez O, Spekreijse H. A spectral compensation method for determining the flicker characteristics of the human colour mechanisms. Vision Res. 1974;14:823–30.
20. Estévez O, Spekreijse H. The "silent substitution" method in visual research. Vision Res. 1982;22:681–91.
21. Kremers J. The assessment of L- and M-cone specific electroretinographical signals in the normal and abnormal retina. Prog Retin Eye Res. 2003;22:579–605.
22. Shapiro AG, Pokorny J, Smith VC. Cone-rod receptor spaces with illustrations that use the CRT phosphor and light-emitting-diode spectra. J Opt Soc Am A. 1996;13:2319–28.
23. Cao D, Nicandro N, Barrionuevo PA. A five-primary photostimulator suitable for studying intrinsically photosensitive retinal ganglion cell functions in humans. J Vis. 2015;15(1):15.1.27. doi:10.1167/15.1.27.
24. Huchzermeyer C, Schlomberg J, Welge-Lussen U, Berendschot TT, Pokorny J, Kremers J. Macular pigment optical density measured by heterochromatic modulation photometry. PLoS One. 2014;9(10):e110521. doi:10.1371/journal.pone.0110521.
25. Bone RA, Landrum JT, Cains A. Optical density spectra of the macular pigment in vivo and in vitro. Vision Res. 1992;32(1):105–10.
26. Kremers J, Usui T, Scholl HPN, Sharpe LT. Cone signal contributions to electroretinograms in dichromats and trichromats. Invest Ophthalmol Vis Sci. 1999;40:920–30.
27. Usui T, Kremers J, Sharpe LT, Zrenner E. Flicker cone electroretinogram in dichromats and trichromats. Vision Res. 1998;38(21):3391–6.
28. Kremers J, Stepien MW, Scholl HPN, Saito CA. Cone selective adaptation influences L- and M-cone driven signals in electroretinography and psychophysics. J Vis. 2003;3:146–60.
29. Kremers J, Parry NR, Panorgias A, Murray IJ. The influence of retinal illuminance on L- and M-cone driven electroretinograms. Vis Neurosci. 2011;28:129–35. doi:10.1017/S0952523810000556. S0952523810000556 [pii].
30. Park JC, Cao D, Collison FT, Fishman GA, McAnany JJ. Rod and cone contributions to the dark-adapted 15-Hz flicker electroretinogram. Doc Ophthalmol. 2015;130(2):111–9. doi:10.1007/s10633-015-9480-3.
31. Hecht S, Haig C, Chase AM. The influence of light adaptation on subsequent dark adaptation of the eye. J Gen Physiol. 1937;20(6):831–50.
32. Silveira LCL, Grünert U, Kremers J, Lee BB, Martin PR. Comparative anatomy and physiology of the primate retina. In: Kremers J, editor. The primate visual system; a comparative approach. Chichester: Wiley; 2005. p. 127–60.
33. Polyak SL. The retina. Chicago: University of Chicago Press; 1941.

34. Boycott BB, Dowling JE. Organization of the primate retina: light microscopy. Philos Trans R Soc Lond B. 1969;255:109–84.
35. Boycott BB, Wässle H. Morphological classification of bipolar cells of the primate retina. Eur J Neurosci. 1991;3:1069–88.
36. Silveira LC, Perry VH. The topography of magnocellular projecting ganglion cells (M-ganglion cells) in the primate retina. Neuroscience. 1991;40(1):217–37.
37. Röhrenbeck J, Wässle H, Boycott BB. Horizontal cells in the monkey retina: immunocytochemical staining with antibodies against calcium binding proteins. Eur J Neurosci. 1989;1:407–20.
38. Martin PR, Grünert U. Spatial density and immunoreactivity of bipolar cells in the macaque monkey retina. J Comp Neurol. 1992;323(2):269–87. doi:10.1002/cne.903230210.
39. Kouyama N, Marshak DW. Bipolar cells specific for blue cones in the macaque retina. J Neurosci. 1992;12:1233–52.
40. Grünert U, Greferath U, Boycott BB, Wässle H. Parasol (Pα) ganglion-cells of the primate fovea: immunocytochemical staining with antibodies against GABA A-receptors. Vision Res. 1993;33(1):1–14.
41. Wässle H, Grünert U, Martin PR, Boycott BB. Immunocytochemical characterization and spatial distribution of midget bipolar cells in the macaque monkey retina. Vision Res. 1994;34:561–79.
42. Watanabe M, Rodieck RW. Parasol and midget ganglion cells of the primate retina. J Comp Neurol. 1989;289:434–54.
43. Dacey DM, Petersen MR. Dendritic field size and morphology of midget and parasol ganglion cells of the human retina. Proc Natl Acad Sci U S A. 1992;89:9666–70.
44. Dacey DM, Lee BB. The 'blue-on' opponent pathway in primate retina originates from a distinct bistratified ganglion cell type. Nature. 1994;367:731–5.
45. Dacey DM, Lee BB, Stafford DM, Smith VC, Pokorny J. Horizontal cells of the primate retina: cone specificity without cone opponency. Science. 1996;271:656–8.
46. Dacey DM, Peterson BB, Robinson FR, Gamlin PD. Fireworks in the primate retina: in vitro photodynamics reveals diverse LGN-projecting ganglion cell types. Neuron. 2003;37(1):15–27.
47. Kolb H, Mariani A, Gallego A. A second type of horizontal cell in the monkey retina. J Comp Neurol. 1980;189:31–44.
48. Kolb H, Linberg K, Fisher SK. Neurons of the human retina: a Golgi study. J Comp Neurol. 1992;318:147–87.
49. Kolb H, Fernandez E, Schouten J, Ahnelt P, Linberg KA, Fisher SK. Are there three types of horizontal cell in the human retina? J Comp Neurol. 1994;343:370–86.
50. Ahnelt PK, Kolb H. Horizontal cells and cone photoreceptors in human retina: a Golgi-electron microscopic study of spectral connectivity. J Comp Neurol. 1994;343:406–27.
51. Boycott BB, Kolb H. The horizontal cells of the rhesus monkey retina. J Comp Neurol. 1973;148:91–114.
52. Boycott BB, Hopkins JM, Sperling HG. Cone connections of the horizontal cells of the rhesus monkey's retina. Proc R Soc Lond B. 1987;229:345–79.
53. Ahnelt P, Kolb H. Horizontal cells and cone photoreceptors in primate retina: a Golgi-light microscopic study of spectral connectivity. J Comp Neurol. 1994;343(3):387–405. doi:10.1002/cne.903430305.
54. Goodchild AK, Chan TL, Grünert U. Horizontal cell connections with short-wavelength-sensitive cones in macaque monkey retina. Vis Neurosci. 1996;13:833–45.
55. dos Reis JW, de Carvalho WA, Saito CA, Silveira LC. Morphology of horizontal cells in the retina of the capuchin monkey, Cebus apella: how many horizontal cell classes are found in dichromatic primates? J Comp Neurol. 2002;443(2):105–23.
56. Dos Santos SN, Dos Reis JWL, da Silva-Filho M, Kremers J, Silveira LCL. Horizontal cell morphology in nocturnal and diurnal primates: a comparison between owl-monkey (Aotus) and capuchin monkey (Cebus). Vis Neurosci. 2005;22:405–15.

57. Peichl L. Morphology of interneurons: horizontal cells. In: Dartt DA, editor. Encyclopedia of the eye. Oxford: Academic; 2010. p. 74–82.
58. Dacheux RF, Raviola E. Horizontal cells in the retina of the rabbit. J Neurosci. 1982;2:1486–93.
59. Bloomfield SA, Miller RF. A physiological and morphological study of the horizontal cell types of the rabbit retina. J Comp Neurol. 1982;208:288–303.
60. Dorgau B, Herrling R, Schultz K, Greb H, Segelken J, Stroh S, et al. Connexin50 couples axon terminals of mouse horizontal cells by homotypic gap junctions. J Comp Neurol. 2015. doi:10.1002/cne.23779.
61. Thoreson WB, Mangel SC. Lateral interactions in the outer retina. Prog Retin Eye Res. 2012;31(5):407–41. doi:10.1016/j.preteyeres.2012.04.003.
62. Chan TL, Goodchild AK, Martin PR. The morphology and distribution of horizontal cells in the retina of a New World monkey, the marmoset Callithrix jacchus: a comparison with macaque monkey. Vis Neurosci. 1997;14:125–40.
63. Chan TL, Grunert U. Horizontal cell connections with short wavelength-sensitive cones in the retina: a comparison between New World and Old World primates. J Comp Neurol. 1998;393(2):196–209.
64. Svaetichin G, MacNichol EF. Retinal mechanisms for chromatic and achromatic vision. Ann N Y Acad Sci. 1958;74:385–404.
65. Ammermüller J, Kolb H. Functional architecture of the turtle retina. Prog Retin Eye Res. 1996;15:393–433.
66. Kolb H, Boycott BB, Dowling JE. A second type of midget bipolar cell in the primate retina. Philos Trans R Soc Lond B. 1969;255:177–80.
67. Kolb H. Organization of the outer plexiform layer of the primate retina: electron microscopy of Golgi-impregnated cells. Philos Trans R Soc Lond B. 1970;258:261–83.
68. Mariani AP. Giant bistratified bipolar cells in monkey retina. Anat Rec. 1983;206:215–20.
69. Mariani AP. Bipolar cells in monkey retina selective for the cone likely to be blue-sensitive. Nature. 1984;308:184–6.
70. Chan TL, Martin PR, Clunas N, Grunert U. Bipolar cell diversity in the primate retina: morphologic and immunocytochemical analysis of a new world monkey, the marmoset Callithrix jacchus. J Comp Neurol. 2001;437(2):219–39.
71. Grünert U, Martin PR, Wassle H. Immunocytochemical analysis of bipolar cells in the macaque monkey retina. J Comp Neurol. 1994;348(4):607–27. doi:10.1002/cne.903480410.
72. Weltzien F, Percival KA, Martin PR, Grünert U. Analysis of bipolar and amacrine populations in marmoset retina. J Comp Neurol. 2015;523(2):313–34. doi:10.1002/cne.23683.
73. Chan TL, Martin PR, Grunert U. Immunocytochemical identification and analysis of the diffuse bipolar cell type DB6 in macaque monkey retina. Eur J Neurosci. 2001;13(4):829–32.
74. Silveira LCL, Lee BB, Yamada ES, Kremers J, Hunt DM. Post-receptoral mechanisms of colour vision in new world primates. Vision Res. 1998;38(21):3329–37.
75. Lameirao SV, Hamassaki DE, Rodrigues AR, DE Lima SM, Finlay BL, Silveira LC. Rod bipolar cells in the retina of the capuchin monkey (Cebus apella): characterization and distribution. Vis Neurosci. 2009;26(4):389–96. doi:10.1017/S0952523809990186.
76. Martin PR, Lee BB, White AJ, Solomon SG, Ruttiger L. Chromatic sensitivity of ganglion cells in the peripheral primate retina. Nature. 2001;410(6831):933–6. doi:10.1038/35073587.
77. Rodieck RW. The primate retina. Comparative primate biology. Neuroscience. 1988;4:203–78.
78. Joo HR, Peterson BB, Haun TJ, Dacey DM. Characterization of a novel large-field cone bipolar cell type in the primate retina: evidence for selective cone connections. Vis Neurosci. 2011;28(1):29–37. doi:10.1017/S0952523810000374.
79. Haverkamp S, Grünert U, Wassle H. The cone pedicle, a complex synapse in the retina. Neuron. 2000;27(1):85–95.

80. Puthussery T, Venkataramani S, Gayet-Primo J, Smith RG, Taylor WR. $Na_V1.1$ channels in axon initial segments of bipolar cells augment input to magnocellular visual pathways in the primate retina. J Neurosci. 2013;33(41):16045–59. doi:10.1523/JNEUROSCI.1249-13.2013.
81. Puthussery T, Percival KA, Venkataramani S, Gayet-Primo J, Grünert U, Taylor WR. Kainate receptors mediate synaptic input to transient and sustained OFF visual pathways in primate retina. J Neurosci. 2014;34(22):7611–21. doi:10.1523/JNEUROSCI.4855-13.2014.
82. Puthussery T, Gayet-Primo J, Taylor WR, Haverkamp S. Immunohistochemical identification and synaptic inputs to the diffuse bipolar cell type DB1 in macaque retina. J Comp Neurol. 2011;519(18):3640–56. doi:10.1002/cne.22756.
83. Lee SC, Jusuf PR, Grunert U. S-cone connections of the diffuse bipolar cell type DB6 in macaque monkey retina. J Comp Neurol. 2004;474(3):353–63. doi:10.1002/cne.20139.
84. Lee SC, Grünert U. Connections of diffuse bipolar cells in primate retina are biased against S-cones. J Comp Neurol. 2007;502(1):126–40. doi:10.1002/cne.21284.
85. Hartline HK. The response of single optic nerve fibers of the vertebrate eye to illumination of the retina. Am J Physiol. 1938;121:400–15.
86. Kuffler SW. Discharge patterns and functional organization of mammalian retina. J Neurophysiol. 1953;16:37–68.
87. Nakanishi S. Second-order neurones and receptor mechanisms in visual- and olfactory-information processing. Trends Neurosci. 1995;18(8):359–64.
88. Slaughter MM, Miller RF. An excitatory amino acid antagonist blocks cone input to sign-conserving second-order retinal neurons. Science. 1983;219(4589):1230–2.
89. Slaughter MM, Miller RF. 2-Amino-4-phosphonobutyric acid: a new pharmacological tool for retina research. Science. 1981;211(4478):182–5.
90. Lee BB, Martin PR, Valberg A. The physiological basis of heterochromatic flicker photometry demonstrated in the ganglion cells of the macaque retina. J Physiol. 1988;404:323–47.
91. Kaiser PK, Lee BB, Martin PR, Valberg A. The physiological basis of the minimally distinct border demonstrated in the ganglion cells of the macaque retina. J Physiol. 1990;422:153–83.
92. Kremers J, Lee BB, Kaiser PK. Sensitivity of macaque retinal ganglion cells and human observers to combined luminance and chromatic modulation. J Opt Soc Am A. 1992;9:1477–85.
93. Maunsell JHR, Nealey TA, DePriest DD. Magnocellular and parvocellular contributions to responses in the middle temporal visual area (MT) of the macaque monkey. J Neurosci. 1990;10(10):3323–34.
94. Lee BB, Wehrhahn C, Westheimer G, Kremers J. Macaque ganglion cell responses to stimuli that elicit hyperacuity in man: detection of small displacements. J Neurosci. 1993;13(3):1001–9.
95. Lee BB, Wehrhahn C, Westheimer G, Kremers J. The spatial precision of macaque ganglion cell responses in relation to Vernier acuity of human observers. Vision Res. 1995;35(19):2743–58.
96. Ruttiger L, Lee B, Sun H. Transient cells can be neurometrically sustained: the positional accuracy or retinal signals to moving targets. J Vis. 2002;2(3):232–42. doi:10.1167/2.3.3.
97. Lee BB, Martin PR, Valberg A, Kremers J. Physiological mechanisms underlying psychophysical sensitivity to combined luminance and chromatic modulation. J Opt Soc Am A. 1993;10:1403–12.
98. Lee BB, Kremers J, Yeh T. Receptive fields of primate retinal cells studied with a novel technique. Vis Neurosci. 1998;15:161–75.
99. Martin PR, Blessing EM, Buzas P, Szmajda BA, Forte JD. Transmission of colour and acuity signals by parvocellular cells in marmoset monkeys. J Physiol. 2011;589(Pt 11):2795–812. doi:10.1113/jphysiol.2010.194076.
100. Livingstone MS, Hubel DH. Psychophysical evidence for separate channels for the perception of form, color, movement, and depth. J Neurosci. 1987;7(11):3416–68.

101. Livingstone MS, Hubel DH. Segregation of form, color, movement, and depth: anatomy, physiology, and perception. Science. 1988;240:740–9.
102. Martin PR. Colour processing in the primate retina: recent progress. J Phsyiol (London). 1998;513(3):631–8.
103. Wiesel TN, Hubel DH. Spatial and chromatic interactions in the lateral geniculate body of the rhesus monkey. J Neurophysiol. 1966;29:1115–56.
104. McCulloch DL, Marmor MF, Brigell MG, Hamilton R, Holder GE, Tzekov R, et al. ISCEV Standard for full-field clinical electroretinography (2015 update). Doc Ophthalmol. 2015;130(1):1–12. doi:10.1007/s10633-014-9473-7.
105. Frishman LJ. Origins of the electroretinogram. In: Heckenlively JR, Arden GB, editors. Principles and practice of clinical electrophysiology of vision. Cambridge, London: The MIT Press; 2006. p. 139–83.
106. Sustar M, Hawlina M, Brecelj J. ON- and OFF-response of the photopic electroretinogram in relation to stimulus characteristics. Doc Ophthalmol. 2006;113:43–52.
107. Pangeni G, Lammer R, Tornow RP, Horn FK, Kremers J. On- and off-response ERGs elicited by sawtooth stimuli in normal subjects and glaucoma patients. Doc Ophthalmol. 2012. doi:10.1007/s10633-012-9323-4.
108. Viswanathan S, Frishman LJ, Robson JG. The uniform field and pattern ERG in macaques with experimental glaucoma: removal of spiking activity. Invest Ophthalmol Vis Sci. 2000;41(9):2797–810.
109. Viswanathan S, Frishman LJ, Robson JG, Harwerth RS, Smith Iii EL. The photopic negative response of the macaque electroretinogram: reduction by experimental glaucoma. Invest Ophthalmol Vis Sci. 1999;40(6):1124–36.
110. Viswanathan S, Frishman LJ, Robson JG, Walters JW. The photopic negative response of the flash electroretinogram in primary open angle glaucoma. Invest Ophthalmol Vis Sci. 2001;42(2):514–22.
111. Armington JC. The electroretinogram. New York: Academic; 1974.
112. Jacobs GH. The discovery of spectral opponency in visual systems and its impact on understanding the neurobiology of color vision. J Hist Neurosci. 2014;23(3):287–314. doi:10.1080/0964704X.2014.896662.
113. Riggs LA, Johnson EP, Schick AM. Electrical responses of the human eye to changes in wavelength of the stimulating light. J Opt Soc Am. 1966;56:1621–7.
114. Riggs LA, Sternheim CE. Human retinal and occipital potentials evoked by changes of the wavelength of the stimulating light. J Opt Soc Am. 1969;59(5):635–40.
115. Sperling HG, Harwerth RS. Red-green cone interaction in the increment-threshold spectral sensitivity of primates. Science. 1971;172:180–4.
116. Harwerth RS, Sperling HG. Effects of intense visible radiation on the increment-threshold spectral sensitivity of the rhesus monkey eye. Vision Res. 1975;15:1193–204.
117. Mills SL, Sperling HG. Red/green opponency in the rhesus macaque ERG spectral sensitivity is reduced by bicuculline. Vis Neurosci. 1990;5:217–21.
118. Sperling HG, Mills SL. Red-green interactions in the spectral sensitivity of primates as derived from ERG and behavioral data. Vis Neurosci. 1991;7:75–86.
119. van Norren D, Baron WS. Increment spectral sensitivities of the primate late receptor potential and b-wave. Vision Res. 1977;17(7):807–10.
120. King-Smith PE, Carden D. Luminance and opponent-color contributions to visual detection and adaptation and to temporal and spatial integration. J Opt Soc Am. 1976;66:709–17.
121. Bush RA, Sieving PA. Inner retinal contributions to the primate photopic fast flicker electroretinogram. J Opt Soc Am A. 1996;13(3):557–65.
122. Armington JC. Chromatic and short term dark adaptation of the human electroretinogram. J Opt Soc Am. 1959;49:1169–75.
123. DeValois RL, Abramov I, Jacobs GH. Analysis of response patterns of LGN cells. J Opt Soc Am. 1966;56:966–77.
124. Baron WS. Cone difference signal in foveal local electroretinogram of primate. Invest Ophthalmol Vis Sci. 1980;19(12):1442–8.

125. Donovan WJ, Baron WS. Identification of the R-G-cone difference signal in the corneal electroretinogram of the primate. J Opt Soc Am A. 1982;72(8):1014–20.
126. Jacobs GH. Primate photopigments and primate color vision. Proc Natl Acad Sci U S A. 1996;93:577–81.
127. Jacobs GH, Deegan Ii JF. Spectral sensitivity of macaque monkeys measured with ERG flicker photometry. Vis Neurosci. 1997;14:921–8.
128. Jacobs GH, Deegan IJS, Moran JL. ERG measurements of the spectral sensitivity of common chimpanzee (Pan troglodytes). Vision Res. 1996;36(16):2587–94.
129. Jacobs GH, Neitz J. Electrophysiological estimates of individual variation in the L/M cone ratio. In: Drum B, editor. Colour vision deficiencies XI. Dordretch: Kluwer; 1993. p. 107–12.
130. Jacobs GH, Neitz J, Krogh K. Electroretinogram flicker photometry and its applications. J Opt Soc Am A. 1996;13(3):641–8.
131. Neitz J, Jacobs GH. Electroretinogram measurements of cone spectral sensitivity in dichromatic monkeys. J Opt Soc Am A. 1984;1:1175–80.
132. Kremers J, Scholl HPN, Knau H, Berendschot TTJM, Usui T, Sharpe LT. L/M cone ratios in human trichromats assesed by psychophysics, electroretinograpy, and retinal densitometry. J Opt Soc Am. 2000;17:517–26.
133. Brainard DH, Roorda A, Yamauchi Y, Calderone JB, Metha AB, Neitz M, et al. Functional consequences of the relative numbers of L and M cones. J Opt Soc Am A. 2000;17(3):607–14.
134. Hofer H, Carroll J, Neitz J, Neitz M, Williams DR. Organization of the human trichromatic cone mosaic. J Neurosci. 2005;25(42):9669–79.
135. Hagstrom SA, Neitz J, Neitz M. Ratio of M/L pigment gene expression decreases with retinal eccentricity. In: Cavonius CR, editor. Colour vision deficiencies XIII. Dordrecht: Kluwer; 1997. p. 59–65.
136. Hagstrom SA, Neitz J, Neitz M. Variation in cone populations for red-green color vision examined by analysis of mRNA. Neuroreport. 1998;9:1963–7.
137. Hagstrom SA, Neitz M, Neitz J. Cone pigment gene expression in individual photoreceptors and the chromatic topography of the retina. J Opt Soc Am A Opt Image Sci Vis. 2000;17(3):527–37.
138. Kuchenbecker JA, Sahay M, Tait DM, Neitz M, Neitz J. Topography of the long- to middle-wavelength sensitive cone ratio in the human retina assessed with a wide-field color multifocal electroretinogram. Vis Neurosci. 2008;25(3):301–6.
139. Jacob MM, Pangeni G, Gomes BD, Souza GS, Da Silva Filho M, Silveira LCL, et al. The spatial properties of L- and M-cone inputs to electroretinograms that reflect different types of post-receptoral processing. PLoS One. 2015;10(3):e0121218. doi:10.1371/journal.pone.0121218.
140. de Lange H. Research into the dynamic nature of the human fovea-cortex systems with intermittent and modulated light. I. Attenuation characteristics with white and colored light. J Opt Soc Am. 1958;48:777–84.
141. Kelly DH, Norren DV. Two-band model of heterochromatic flicker. J Opt Soc Am. 1977;67:1081–91.
142. Kremers J, Link B. Electroretinographic responses that may reflect activity of parvo- and magnocellular post-receptoral visual pathways. J Vis. 2008;8(15/11):1–14.
143. Kremers J, Pangeni G. Electroretinographic responses to photoreceptor specific sine wave modulation. J Opt Soc Am A. 2012;29(2):A309–16.
144. Kommanapalli D, Murray IJ, Kremers J, Parry NR, McKeefry DJ. Temporal characteristics of L- and M-cone isolating steady-state electroretinograms. J Opt Soc Am A Opt Image Sci Vis. 2014;31(4):A113–20. doi:10.1364/JOSAA.31.00A113.
145. Kremers J, Rodrigues AR, Silveira LCL, da Silva-Filho M. Flicker ERGs representing chromaticity and luminance signals. Invest Ophthalmol Vis Sci. 2010;51:577–87.
146. Lee BB, Sun H, Valberg A. Segregation of chromatic and luminance signals using a novel grating stimulus. J Physiol. 2011;589(Pt 1):59–73. doi:10.1113/jphysiol.2010.188862. jphysiol.2010.188862 [pii].

147. Parry NR, Murray IJ, Panorgias A, McKeefry DJ, Lee BB, Kremers J. Simultaneous chromatic and luminance human electroretinogram responses. J Physiol. 2012;590:3141–54. doi:10.1113/jphysiol.2011.226951.
148. Kremers J, Pangeni G, Tsaousis KT, McKeefry D, Murray IJ, Parry NR. Incremental and decremental L- and M-cone driven ERG responses: II. Sawtooth stimulation. J Opt Soc Am A Opt Image Sci Vis. 2014;31(4):A170–8. doi:10.1364/JOSAA.31.00A170.
149. McKeefry D, Kremers J, Kommanapalli D, Challa NK, Murray IJ, Maguire J, et al. Incremental and decremental L- and M-cone-driven ERG responses: I. Square-wave pulse stimulation. J Opt Soc Am A Opt Image Sci Vis. 2014;31(4):A159–69. doi:10.1364/JOSAA.31.00A159.
150. Murray IJ, Kremers J, Parry NRA. L- and M-Cone isolating ergs: LED versus CRT stimulation. Vis Neurosci. 2008;25:327–31.
151. Yamaguchi S, Motulsky AG, Deeb SS. Visual pigment gene structure and expression in human retinae. Hum Mol Genet. 1997;6:981–90.

http://www.springer.com/978-3-319-44976-0

Human Color Vision
Kremers, J.; Baraas, R.C.; Marshall, N.J. (Eds.)
2016, XI, 361 p. 82 illus., 74 illus. in color., Hardcover
ISBN: 978-3-319-44976-0